NASA
Technical
Memorandum

NASA TM - 100375

WIND MODELS FOR THE NSTS ASCENT TRAJECTORY BIASING FOR WIND LOAD ALLEVIATION

By O.E. Smith, S.I. Adelfang, G.W. Batts, and C.K. Hill

Earth Science and Applications Division
Space Science Laboratory
Science and Engineering Directorate

August 1989

NASA

National Aeronautics and
Space Administration

George C. Marshall Space Flight Center

1. REPORT NO. NASA TM--100375	2. GOVERNMENT ACCESSION NO.	3. RECIPIENT'S CATALOG NO.

4. TITLE AND SUBTITLE Wind Models for the NSTS Ascent Trajectory Biasing for Wind Load Alleviation	5. REPORT DATE August 1989
	6. PERFORMING ORGANIZATION CODE

7. AUTHOR(S) O.E. Smith,* S.I. Adelfang,* G.W. Batts,* and C.K. Hill	8. PERFORMING ORGANIZATION REPORT #

9. PERFORMING ORGANIZATION NAME AND ADDRESS George C. Marshall Space Flight Center Marshall Space Flight Center, Alabama 35812	10. WORK UNIT NO.
	11. CONTRACT OR GRANT NO.

12. SPONSORING AGENCY NAME AND ADDRESS National Aeronautics and Space Administration Washington, D.C. 20546	13. TYPE OF REPORT & PERIOD COVERED Technical Memorandum
	14. SPONSORING AGENCY CODE

15. SUPPLEMENTARY NOTES

Prepared by Earth Science and Applications Division, Space Science Laboratory, Science and Engineering Directorate.

16. ABSTRACT

This technical report presents new concepts for aerospace vehicle ascent wind profile biasing. The purpose for wind biasing the ascent trajectory is to provide ascent wind loads relief and thus decrease the probability for launch delays due to wind loads exceeding critical limits. Wind biasing trajectories to the profile of monthly mean winds have been widely used for this purpose. The wind profile models presented in this report give additional alternatives for wind biased trajectories. They are derived from the properties of the bivariate normal probability function using the available wind statistical parameters for the launch site. The analytical expressions are presented to permit generalizations. Specific examples are given to illustrate the procedures. The wind profile models can be used to establish the ascent trajectory steering commands to guide the vehicle through the first stage. For the National Space Transportation System (NSTS) program these steering commands are called I-loads.

*Applied Technology Division, Computer Sciences Corp., Huntsville, Alabama 35816.

17. KEY WORDS Wind profiles Bivariate normal Probability functions Steering commands	18. DISTRIBUTION STATEMENT Unclassified – Unlimited

19. SECURITY CLASSIF. (of this report) Unclassified	20. SECURITY CLASSIF. (of this page) Unclassified	21. NO. OF PAGES 58	22. PRICE NTIS

MSFC - Form 3292 (Rev. December 1972)

For sale by National Technical Information Service, Springfield, Virginia 22151

TABLE OF CONTENTS

Page

PRECEDING PAGE BLANK NOT FILMED

iii

PAGE _ii_ INTENTIONALLY BLANK

LIST OF ILLUSTRATIONS

TECHNICAL MEMORANDUM

WIND MODELS FOR THE NSTS ASCENT TRAJECTORY BIASING FOR WIND LOADS ALLEVIATION

I. INTRODUCTION

A. Background

Wind biasing the aerospace vehicle ascent trajectory to the profile of monthly mean wind vectors to provide ascent wind loads relief has been used for many years. The first major NASA project that used this wind biasing technique in both the pitch and yaw planes was Skylab, which was launched in May 1973. Beginning in 1976, the National Space Transportation System (NSTS) Program Office adopted this technique of wind biasing in the ascent trajectory. The monthly mean wind vectors were established at 1-km altitude intervals from 0- to 27-km altitude using 12 years of Rawinsonde wind records for Kennedy Space Center (KSC) and 9 years for Vandenberg Air Force Base (VAFB).

Recently the NSTS Program Office has directed that alternatives be developed for biasing the ascent trajectory to yield ascent wind load relief. The procedure is to establish profiles versus trajectory elapsed time or Mach number for two dynamic load indicators. The dynamic load indicators are the products q·alpha and q·beta; where q is the aerodynamic pressure, alpha is the angle-of-attack in the pitch plane, and beta is the angle of side slip in the yaw plane. The shape of the q·alpha and the q·beta profiles are determined from an engineering analysis of the flight vehicle and the mission. These profiles of q·alpha and q·beta and combinations of both are used to establish the steering commands to guide the vehicle through the first stage. For the NSTS these steering commands are called I-loads. The trajectory that is wind biased to the profile of monthly mean wind vectors is called the baseline I-load. The trajectories for the baseline I-load and up to eight alternate I-loads are used for the performance analysis and the ascent wind loads analysis. This work is done months in advance of the scheduled launch date. The reason for using more than the baseline I-load is to decrease the chances for launch delay due to wind loads exceeding critical limits.

On the day of launch (DOL), rigid body ascent wind loads simulations are performed for the baseline I-load and the alternate I-loads using the measured wind profiles. The I-load that yields the smallest ascent wind loads is selected for use in the launch decision process. This procedure does not ensure a decision to launch because it is conceivable that the wind measured during the countdown could yield load exceedances for all nine I-loads.

There is no specific knowledge of the wind profile shape that produces the alternate I-loads based on the q·alpha and the q·beta techniques. Hence, the following issues are raised:

1. Can wind biasing profile models be developed for alternate I-loads that meet the objective of increasing launch probability?

2. Can a knowledge of the wind profile used for the alternate I-loads be used to an advantage on the DOL?

3. How can the wind biasing profile models be evaluated?

Responses to the above three issues are:

1. Wind profile models for alternate I-loads can be developed to meet the objective of increasing the launch probability due to ascent wind loads. However, these wind models must be evaluated against the current using the q·alpha–q·beta profiles.

2. On the DOL if the measured wind profile has only small deviations from the profile of the monthly mean wind vectors, then it can be anticipated that the baseline I-load would be the choice for the wind bias selection at that time during the countdown and similarly for any other wind-biased trajectory. The task then becomes that of projecting the change in the wind profile with time from the known wind profiles that were used for the development of the alternate I-loads. It is conceivable that the q·alpha–q·beta profile I-load designs could introduce large wind profile shears that are unrealistic due to wind profile changes during the countdown.

3. The wind bias models can be evaluated for steady state time changes using a sample of four times daily (6-hr intervals) taken from an available 5-year period of serially complete Rawinsonde wind records for KSC. A suggested method for this evaluation of wind bias changes is that of finding the nearest profile neighbor. That is, find the best agreement from one wind profile to the next that is nearest to the alternate wind bias profile.

Of greater significance is that the proposed wind profile models will ensure a statistical connection between the in-plane and out-of-plane wind components and thus relate a connection between the two dynamic load indicators, q·alpha and q·beta.

B. Required Statistics for the Wind Bias Models

The bivariate normal probability distribution is used to model the wind vectors at discrete altitudes [1]. The multivariate normal probability distribution is used to develop the NSTS design Synthetic Vector Wind Profile (SVWP) [1]. The SVWP model establishes the design requirements for q·alpha and q·beta. At discrete Mach numbers a graphic display for q·alpha versus q·beta forms a closed curve. This curve is called a "squatchaloid," which is a coined word.

This report uses the bivariate normal probability distribution to model the wind bias profiles. The required five statistical parameters for this distribution are the two monthly component mean values, the two standard deviations, and the correlation coefficient between the components versus altitude. The same data base used for the SVWP model is used for the wind bias models. For KSC this data base is from 12 years of Rawinsonde records that have been made serially complete twice daily from 0- to 27-km altitude at 1-km intervals. For VAFB the wind data is from a 9-year period of record.

The five statistical parameters are tabulated in Reference 2 and are available on computer tapes for each monthly reference period. These five parameters are with respect to the meteorological coordinate system (Fig. 1).
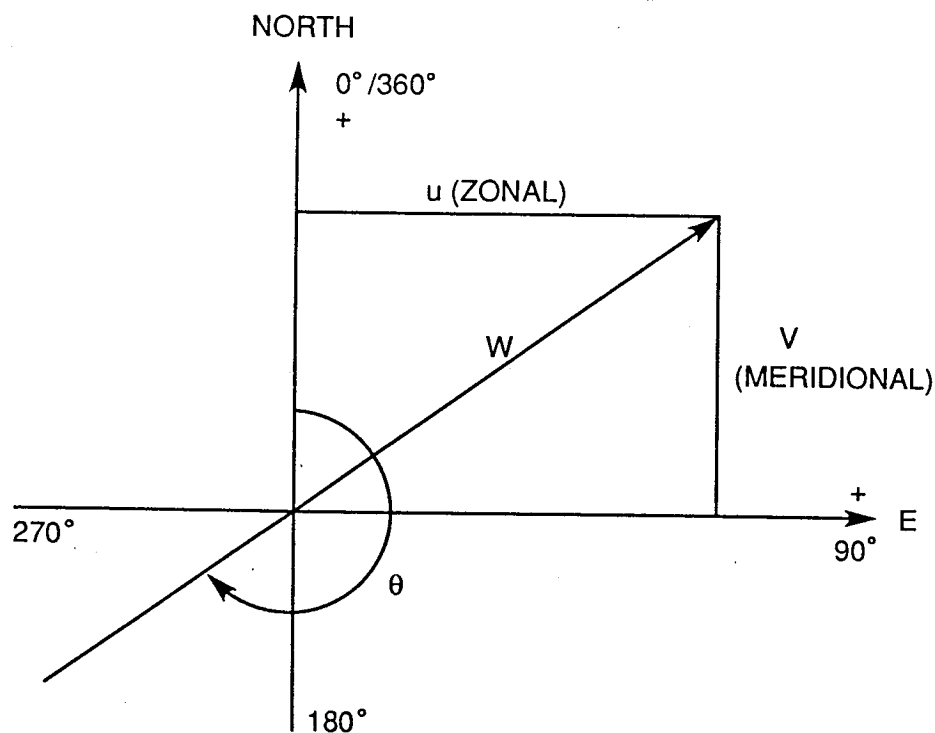
NORTH

0°/360°
+

u (ZONAL)

W

V
(MERIDIONAL)

270°

+
90°
E

θ

180°

Figure 1. Meteorological coordinate system.

Definitions:

U is the zonal wind component, positive west to east in units, m/s.

V is the meridional wind component, positive south to north in units, m/s.

W is wind speed in units, m/s.

θ is the wind direction measured in degrees clockwise from true north and is the direction from which the wind is blowing.

(For the NSTS program, the sign convention for the wind vectors are reversed.)

$$U = -W \cos \theta ,$$
(1)

$$V = -W \sin \theta ,$$
(2)

where $0° \leqslant \theta \leqslant 360°$.

The five wind statistical parameters are:

$\bar{U}$ – the monthly mean zonal wind component (m/s).

$\bar{V}$ – the monthly mean meridional wind component (m/s).

S_u – the standard deviation with respect to the monthly mean for the zonal wind component (m/s).

S_v – the standard deviation with respect to the monthly mean for the meridional wind component (m/s).

$R(U,V)$ – the correlation coefficient between the two components.

By using coordinate rotation equations, these five statistical parameters can be calculated with respect to any orthogonal coordinates. Let the vehicle flight azimuth, α, be measured in degrees clockwise from true north, then the five statistical parameters with respect to the flight axes are given by the following equations:

(a) The means

$$\bar{X}_\alpha = \bar{U} \sin \alpha + \bar{V} \cos \alpha \tag{3}$$

$$\bar{X}_\alpha = \bar{V} \sin \alpha - \bar{U} \cos \alpha \tag{4}$$

(b) The variances

$$S_{x\alpha}^2 = S_u^2 \sin^2 \alpha + S_v^2 \cos^2 \alpha + 2 R(U,V) S_u S_v \sin \alpha \cos \alpha \tag{5}$$

$$S_{y\alpha}^2 = S_v^2 \sin^2 \alpha + S_u^2 \cos^2 \alpha - 2 R(U,V) S_u S_v \sin \alpha \cos \alpha \tag{6}$$

(c) The correlation coefficients

$$R(X,Y)_\alpha = \frac{\text{cov } (X,Y)_\alpha}{S_{x\alpha} S_{y\alpha}} \tag{7}$$

where cov $(X,Y)_\alpha$ is the rotated covariance.

$$\text{cov } (X,Y)_\alpha = R(U,V) S_u S_v (\sin^2\alpha - \cos^2\alpha) + \sin \alpha \cos \alpha (S_v^2 - S_u^2) \ . \tag{8}$$

4

C. The Wind Data Base Used for the NSTS Loads Assessment

For the NSTS a sample of 150 Jimsphere wind profiles per month for KSC are used in a rigid body ascent wind loads simulation using the baseline I-load to determine the percentage of wind profiles that do not yield a load limit for winds on any one of approximately 100 load structural members. The percentage of wind profiles that caused no structural load exceedances is the launch probability for the given month and mission. The structural load limit for wind is determined after accounting for the systems uncertainties (for example, the aerodynamic variations, misalignment, etc.) and the elastic body loads due to wind gust, and the contribution that the wind profile variability with respect to time in 2 hr or 3.5 hr makes to rigid body loads. Those wind profiles that produced load exceedances for the baseline I-load are then reused in loads simulations using the alternate I-loads. Then a composite launch probability is quoted for the baseline I-load and the alternate I-loads. This procedure decreases the probability of a launch delay or scrub due to ascent loads.

II. WIND PROFILE MODELS

A. Profile of Monthly Mean Wind Vectors

The monthly vector mean wind is defined in meteorological terminology as zonal and meridional mean wind components or as the resultant vector magnitude and the resultant direction in polar coordinates. For a bivariate normal probability function, these mean wind vectors are the most likely values to occur at discrete altitudes. In the absence of all other knowledge, these mean winds are the best guess for the month to minimize the wind dispersions at discrete altitudes. It is the profile of monthly mean vectors versus altitude that is used for aerospace vehicle ascent trajectory wind biasing for wind loads alleviation. These mean wind vectors are expressed in polar coordinates for the convenience of flight trajectory analysis.

B. Wind Vectors for Assigned Wind Components to a Probability Ellipse

For this wind profile biasing model four wind vectors are selected. They are the two wind vectors that give the largest head and tail wind components relative to the monthly mean wind and the two wind vectors that give the largest crosswind, left-to-right and right-to-left, relative to the monthly mean wind (Fig. 2). The five bivariate normal statistical parameters for each altitude at 1-km intervals for the month of interest are used. If the flight azimuth is not greatly different from 90° east of north, there is no need to use the coordinate rotation equations for these parameters.

The equations to derive these four wind vectors are expressed in general form. The probability ellipse is arbitrarily chosen. For the example presented in this report the 85-percent probability ellipse has been selected.
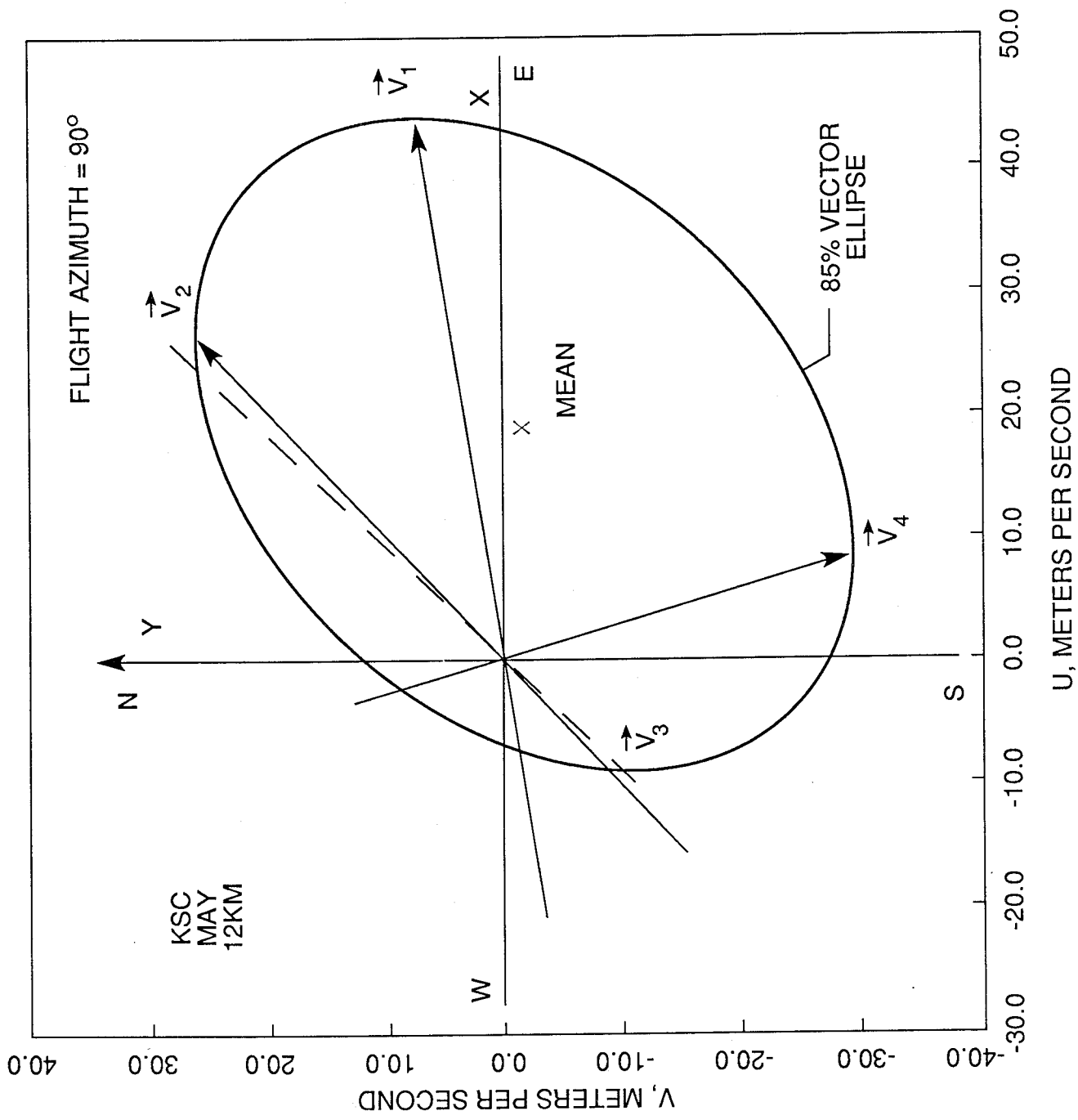
Figure 2. Four selected wind vectors to the 85-percent probability ellipse.

The bivariate normal wind probability ellipse can be written in general form as:

$$AX^2 + BXY + CY^2 + DX + EY + F = 0 \; ,$$
(9)

where

$$A = S_v^2$$

$$B = -2 \, R(U,V) \, S_u \, S_v$$

$$C = S_u^2$$

$$D = -(B \, \bar{V} + 2 \, A \, \bar{U})$$

$$E = -(B \, \bar{U} + 2 \, C \, \bar{V})$$

$$F = A\bar{U}^2 + C\bar{V}^2 + B\bar{U}\bar{V} - AC \{1 - [R(U,V)]^2\} \, \lambda e^2$$

and

$$\lambda e = \sqrt{-2 \, \ln \, (1-P)} \; ,$$

where P is probability. For this wind probability model, P percent of the wind vectors will lie within the assigned probability ellipse.

An example for the 85 percent wind probability ellipse for May at 12-km altitude for KSC is shown in Figure 2 with respect to a 90° flight azimuth. Also illustrated (Fig. 2) are the four wind vectors to the 85-percent ellipse that yield the largest head, tail wind, and crosswind components relative to the monthly mean.

The analytical equations for these four wind components in Cartesian coordinates for a 90° flight azimuth are:

(a) Wind Vector 1

$$X_1 = \bar{U} + \lambda e \, S_u$$
(10.1)

largest relative tailwind

$$Y_1 = \bar{V} + \lambda e \, R(U,V) \, S_v$$
(10.2)

associated crosswind component.

7

(b) Wind Vector 2

$$X_2 = \bar{U} + \lambda e \ R(U.V) \ S_u \qquad (11.1)$$

associated in-plane wind component

$$Y_2 = \bar{V} + \lambda e \ S_v \qquad (11.2)$$

largest right-to-left crosswind component.

(c) Wind Vector 3

$$X_3 = \bar{U} - \lambda e \ S_u \qquad (12.1)$$

largest relative head wind component

$$Y_3 = \bar{V} - \lambda e \ R(U.V) \ S_v \qquad (12.2)$$

associated crosswind component.

(d) Wind Vector 4

$$X_4 = \bar{U} - \lambda e \ R(U,V) \ S_u \qquad (13.1)$$

associated in-plane wind component

$$Y_4 = \bar{V} - \lambda e \ S_v \qquad (13.2)$$

the largest left-to-right crosswind component.

The above simple equations [equations (10)–(13)] were derived from equation (9).

The wind vectors are put in polar form using the meteorological convention of wind speed, W, and wind direction, θ.

$$W = \sqrt{X^2 + Y^2} \qquad (14)$$

$$\theta = \tan^{-1} (v/u) + \text{quadrant correction} \ . \qquad (15)$$

8

On the Selection of the Probability Ellipse

A rationale for the choice of probability ellipse is given. The probability level selected for the wind vector ellipse should be the one where the wind vectors that intercept the probability ellipse are greatly different from the monthly mean and where a discrimination can be made between the wind vectors due to changes with time. For this report the 85-percent wind probability ellipse was selected (Fig. 3). In Figure 3 the 12-hr and 24-hr time conditional 50-percent probability ellipses are illustrated. The given wind vectors are the four wind vectors that yield the largest relative head-tail wind and crosswind components. For the 12-hr time conditional 50-percent ellipses there are no common areas for the four given wind vectors. The time conditional probability ellipses are based on the 14 quadravariate probability parameters [3]. From Figure 3 it would be appealing to introduce additional wind vectors including one between wind vectors $\vec{V}_2$ and $\vec{V}_3$, and one between $\vec{V}_4$ and $\vec{V}_1$. A generalization describing how to do this is presented at the end of this section.

Another justification for selecting the 85-percent probability is based on the univariate normal probability function for the components. For the 85-percent probability ellipse, $P = 0.85$,

$$\lambda e = \sqrt{-2 \ln (1 - P)} \quad , \tag{16}$$

for $P = 0.85$, this gives $\lambda e = 1.9479$. This is used as a t-value of 1.9479 for the univariate normal probability.

For the defined wind components

$$\Pr \{X \leqslant X_1\} = 0.9745 \tag{17}$$

that is, X_1 is the 97.45 percentile value.

$$\Pr \{X \leqslant X_3\} = 0.0255 \tag{18}$$

and

$$\Pr \{X_3 \leqslant X \leqslant X_1\} = 0.949 \quad . \tag{19}$$

This is the 94.9 interpercentile range. The probabilities for the Y-wind components are

Figure 3. Example for 50-percent time conditional wind probability ellipses for 12 and 24 hours for given vectors.

$$\Pr \{Y \leq Y_2\} = 0.9745 \tag{20}$$

$$\Pr \{Y \leq Y_4\} = 0.0255 \tag{21}$$

and

$$\Pr \{Y_4 \leq Y \leq Y_2\} = 0.949 \quad . \tag{22}$$

For a larger probability ellipse, the interpercentile range for these wind components would increase.

There is an analytical statistical connection between the wind component for the four selected vectors as defined by equations (10) through (13). This connection is from the conditional probability function for bivariate normal variates.

The expected value or conditional mean values are:

$$E(Y|X^*) = \bar{Y} + R(U,V) (S_v/S_u) (X^* - \bar{X}) \tag{23}$$

$$E(X|Y^*) = \bar{X} + R(U,V) (S_u/S_v) (Y^* - \bar{Y}) \quad . \tag{24}$$

The conditional standard deviations are:

$$S(Y|X^*) = S_v \sqrt{1 - [R(U,V)]^2} \tag{25}$$

$$S(X|Y^*) = S_u \sqrt{1 - [R(U,V)]^2} \quad . \tag{26}$$

Comparing equations (23) through (26) with equations (10) through (13), it is seen that the asssociated wind component for Y_1 for X_1 [equation (10)] is the conditional mean, i.e., the best estimate or most likely value for Y given X_1. In similar manner the other conditional means are

$$E(X_2|Y_2) \quad , \quad E(Y_3|X_3) \quad , \quad \text{and} \quad E(X_4|y_4) \quad .$$

Equations (23) and (25) are also regression functions which are linear functions of X and Y, respectively. For a bivariate normal distribution, the conditional parameter estimates are the same as those derived by the method of least squares. An example for the conditional means compared with the 50, 75, 85, and 95 percent probability ellipses is shown in Figure 4. The significance of the relationship between the wind components for the assigned wind vectors as defined by equations (10) through (13) when applied as a wind biasing profile model is that there is a connection between the in-plane and out-of-plane trajectory parameters for q·alpha and q·beta. This is a primary argument in favor of the advocated wind modeling technique for the alternate I-load design.
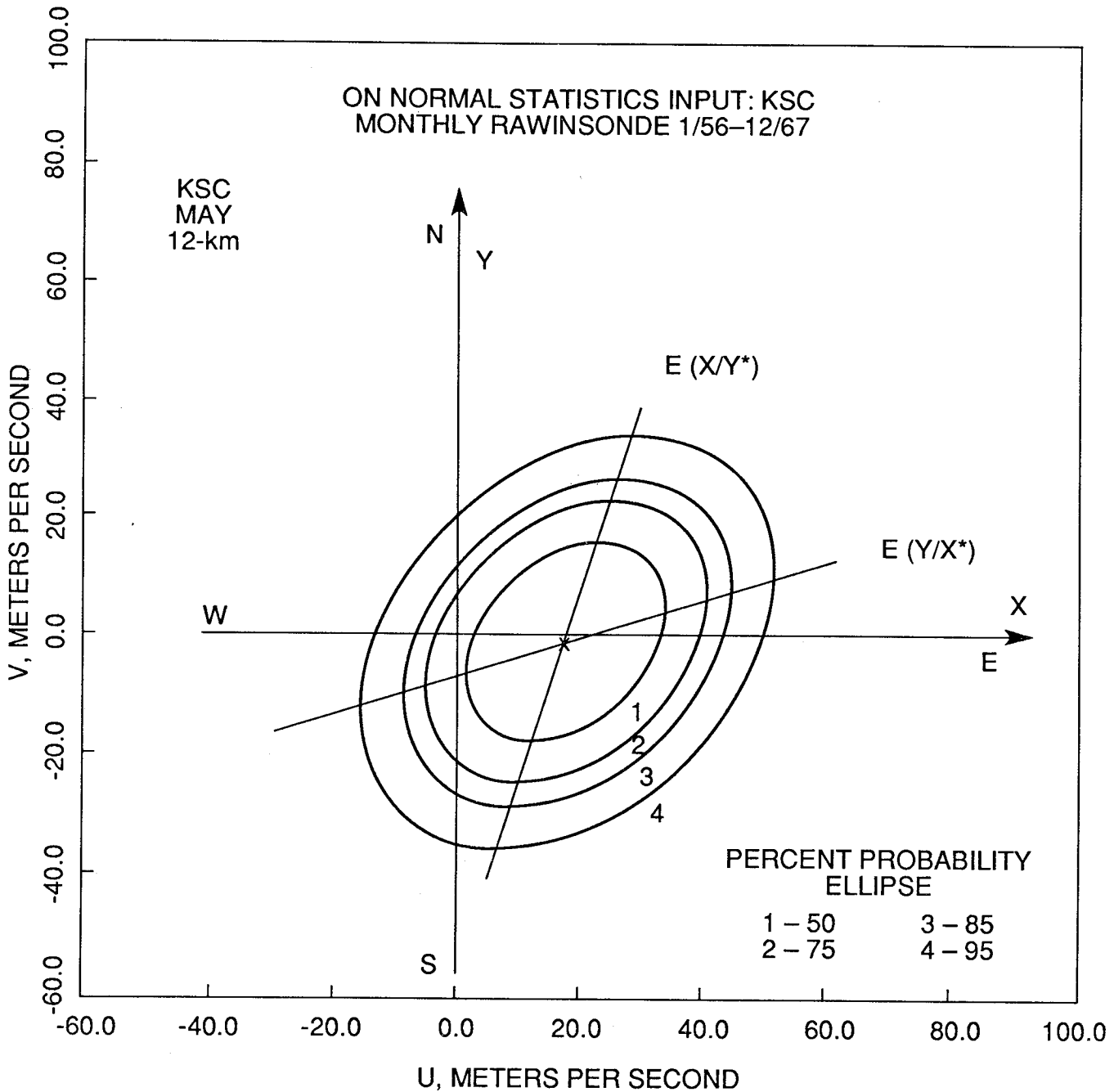

Figure 4. Conditional mean wind component versus given wind component.

A Generalized Expression for the Wind Vectors to a Probability Ellipse

The wind vectors relative to the monthly mean, R, to an assigned probability ellipse for any arbitrary clocking angle, ψ, can be computed from the conditional bivariate normal probability function written in polar coordinates [1].

The conditional probability for, R, given ψ (Fig. 5) is:

$$\Pr \{R \leq R^*|\psi\} = 1 - \exp[-A^2 R^2/2] \tag{27}$$

where

$$A^2 = \frac{1}{[1 - \{R(U,V)\}^2]} \left[\frac{\cos^2\psi}{S_u^2} - \frac{2\,R(U,V)\,\cos\psi\,\sin\psi}{S_u\,S_v} + \frac{\sin^2\psi}{S_v^2} \right]$$

Solving equation (27) for R* yields

$$R^* = \sqrt{-2\,\ln\,(1-P)} \Big/ A = \lambda e/A \quad . \tag{28}$$
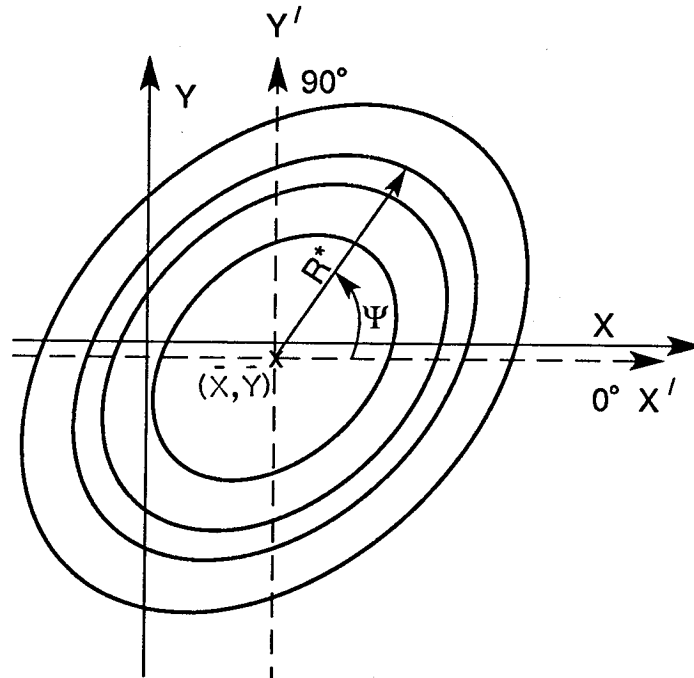

Figure 5. Definitions for any wind vector relative to the monthly mean to a probability ellipse.

13

The wind vector components are given by

$$X = \bar{X} + (\lambda e/A) \cos \psi \qquad (29)$$

$$Y = \bar{Y} + (\lambda e/A) \sin \psi \qquad (30)$$

Equations (28) through (30) could be used to compute the wind vectors that lie between the four selected vectors previously described in Figure 2.

C. Wind Vectors to the Major and Minor Axes to the Bivariate Normal Probability Ellipse

The equations used to compute the four wind vectors that intercept the elliptic major and minor axes of the probabilty ellipse are presented in Figure 6. (The suggestion for this model is from a private communication with H. Cordova, Rockwell Space Operations Company.)
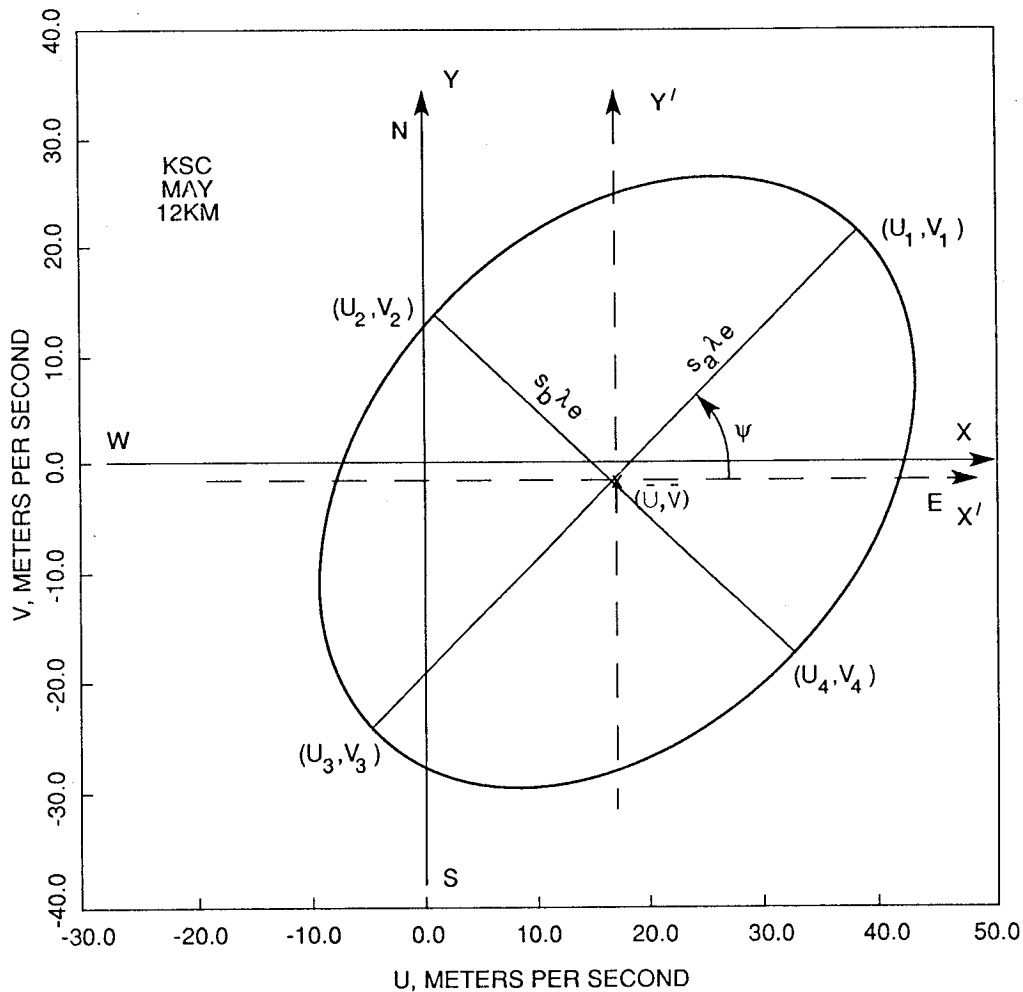

Figure 6. Wind vectors to semi-major and semi-minor axes to a probabilty ellipse.

The standard deviations of the wind components along the major axis, S_A, and the minor axis, S_B, to the probability ellipse are given by:

$$S_A = \{\tfrac{1}{2} [(S_u^2 + S_v^2) + q]\}^{1/2}$$

(31)

$$S_B = \{\tfrac{1}{2} [(S_u^2 + S_v^2) - q]\}^{1/2}$$

(32)

where

$$q = \sqrt{(S_u^2 + S_v^2)^2 - 4 S_u^2 S_v^2 \{1-[R(U,V)]^2\}} \quad .$$

The angle, ψ, between the X-axis and the major elliptic axis (Fig. 6) is given by:

$$\psi = 1/2 \tan^{-1}\left(\frac{2 R(U,V) S_u S_v}{|S_u^2 - S_v^2)|}\right)$$

(33)

$-90° \leq \psi \leq 90°$.

It is noted that equation (33) also gives the coordinate rotation angle required to yield a zero correlation coefficient for the bivariate normal probability distribution.

The wind components from the centroid of the probability ellipse to the intercept of the major and minor axes to the probability ellipse are:

For the major axis,

$$U_A = \lambda e \, S_A \cos \psi$$

(34)

$$V_A = \lambda e \, S_A \sin \psi$$

(35)

and for the minor axis,

$$U_B = \lambda e \, S_B \sin \psi$$

(36)

$$V_B = \lambda e \, S_B \cos \psi$$

(37)

where

$$\lambda e = \sqrt{-2 \ln (1-P)} \tag{38}$$

and P is the probability.

The four wind vectors to the major and minor axes for the probability ellipse in the meteorological Cartesian coordinate system with respect to the origin are given by:

$$U_1 = \bar{U} + U_A \tag{39.1}$$

$$V_1 = \bar{V} + V_A \tag{39.2}$$

$$U_3 = \bar{U} - U_A \tag{40.1}$$

$$V_3 = \bar{V} - V_A \tag{40.2}$$

$$U_2 = \bar{U} - U_B \tag{41.1}$$

$$V_2 = \bar{V} + V_B \tag{41.2}$$

$$U_4 = \bar{U} + U_B \tag{42.1}$$

$$V_4 = \bar{V} - V_B \tag{42.2}$$

The above four wind vectors in the meteorological polar coordinate system are given by:

$$W = \sqrt{U^2 + V^2} \ , \tag{43}$$

where W is the wind speed and

$$\theta = \tan^{-1} (V/U) + \text{quadrant correction} \ . \tag{44}$$

The angle, θ, is the direction from which the wind is blowing measured in degrees clockwise from true north.

16

If it is desired to find the four wind vectors to the probability ellipse that lie half-way between the semi-major and semi-minor axes, define the angles of rotation, φ, in degrees by:

$$\varphi_N = \psi + (2n-1)\,\pi/4 \quad,$$

(45)

where n = 1, 2, 3, and 4, and ψ is from equation (33).

Use φ_N in equations (34) through (38) to compute these four intermediate wind vectors.

The combined procedures yield eight specific wind vectors to the probability ellipse that have a 45° increment with respect to the centroid of the probability ellipse that begins with the first semi-major axis.

The Largest and Smallest Wind Vector to a Probability Ellipse

It is obvious that semi-major and semi-minor axes (Fig. 6) to a probability ellipse give the largest and smallest wind vectors relative to the monthly mean. No generalized closed form expression for the largest and smallest wind vectors measured from the X-Y origin (Fig. 6) to an arbitrary bivariate normal probability ellipse has been found, except for the special case of the bivariate circular normal probability function.

III. ILLUSTRATIVE EXAMPLES

This section presents the wind vectors to the 85-percent probability ellipse defined by the components (Section II.B) and the wind vectors to the major and minor axes of the 85-percent ellipse (Section II.C). These examples are illustrated for May wind data for KSC in Appendix A and Appendix B.

A. Profiles of Wind Vectors for Assigned Wind Components to the 85-Percent Probability Ellipse

Table A-1 contains the five bivariate normal wind statistical parameters for May at KSC. This table, from Reference 2, is based on a 12-year period of Rawinsonde wind records for KSC. These statistical parameters are all that are required to derive the many wind probability models that can be developed using the properties of the bivariate normal probability function.

Table A-2 contains the four wind vectors in Cartesian coordinates that produce the largest head, tail, and crosswind components relative to the monthly mean wind to the 85-percent probability ellipse for a vehicle flight azimuth of 90°. Table A-2 is computed using equations (10) through (13). The input parameters are from Table A-1.

17

Table A-3 contains the four wind vectors from Table A-2 and the monthly mean wind vectors from Table A-1, put in the meteorological polar coordinate system using equations (14) and (15). This table contains the wind profiles to establish the baseline I-load and the four alternate I-loads.

Figures A-1 through A-4 present the wind vector profiles in Cartesian coordinates for the profile of monthly means and four selected wind vectors using the data contained in Table A-2. These selected wind biasing profiles are for the four alternate I-loads. These four wind profile models have smooth variations with altitude similar to the profiles of monthly mean wind vectors.

Figures A-5 through A-12 are illustrations for wind speed and wind direction versus altitude for the four wind profiles from Table A-3, compared with the monthly mean resultant wind speed and the resultant wind direction. These figures are plotted from the data contained in Table A-3.

B. Profile of Wind Vectors to the Major and Minor Axes of the 85-Percent Probability Ellipse

Table B-1 contains the four wind vectors in Cartesian coordinates to the major and minor axes of the 85-percent probability ellipse using equations (31) through (42) where the input parameters are from Table A-1. These four wind vector profiles are illustrated in Figures B-1 through B-4 and compared with the profile of monthly mean wind components taken from Table A-1.

Table B-2 contains the four wind vector profiles given in Table B-2 but presented in the meteorological polar coordinate system. These four wind profiles are illustrated as wind speed and wind direction in Figures B-5 through B-12.

IV. CONCLUSIONS

Statistical wind profile models for the purpose of wind biasing aerospace vehicle ascent trajectories to provide structural wind loads alleviations have been developed.

These wind vector profile models are derived from the properties of the bivariate normal probability function. Two methods have been presented. The first method is the selection of wind vectors to a probability ellipse that gives the largest head, tail, right and left crosswind components relative to the monthly mean wind. This selection of wind vectors is a highly significant feature of this model because there is an analytical probability connection between the wind components for the defined vectors. This connection is that one component is the conditional mean given the other and further the conditional means also form the linear regression for the bivariate normal distribution. Hence, in applications for the NSTS alternate I-loads design there should be a connection between the trajectory parameters in the pitch and the yaw planes.

The second method is the selection of wind vectors that intercept the semi-major and semi-minor axes at the assigned probability ellipse. This method is appealing because the wind vector directions relative to the monthly mean to the probability ellipse are at right angles. The wind vectors along the semi-major and semi-minor axes have the largest and smallest magnitudes relative to the monthly mean.

The analytical functions for these wind profile biasing models have been presented to facilitate generalization on these models. The choice of the 85-percent vector wind ellipse used to illustrate the principles for the wind models is arbitrary. From ascent wind loads simulations, a better choice for the reference probability ellipse may be found to decrease the overall probability for launch delay or scrub due to ascent wind loads restrictions.

The wind profile models for alternate I-loads design are simple to compute. If the wind profile models are used for the I-load design, an advantage of this information can be made on the DOL in monitoring the wind profile. On the other hand, the design of the alternate I-load based on the q·alpha and q·beta profiles does not provide a definite knowledge of the equivalent wind profiles. No procedure has been established to calculate the equivalent wind profiles from the q·alpha and q·beta profiles used for the alternate I-loads. There may not be unique wind profiles that produce the q·alpha and q·beta profiles.

REFERENCES

1. Smith, O.E.: Vector Wind and Vector Wind Shear Models 0–27 km Altitude for Cape Kennedy, Florida, and Vandenberg AFB, California. NASA TMX-73319, July 1976.

2. Falls, L.W.: Normal Probabilities for Cape Kennedy Wind Components – Monthly Reference Periods for All Flight Azimuths – Altitudes 0 to 70 Kilometers. NASA TMX-64771, April 16, 1973.

3. Adelfang, S.I.: Analysis of Vector Wind Changes with Respect to Time for Cape Kennedy, Florida. NASA CR-150779, August 1978.

APPENDIX A

TABLE A-1. ZONAL AND MERIDIONAL WIND COMPONENT
STATISTICAL PARAMETERS
(Valid for Vehicle Flight Azimuth of 90°, May, KSC)

Altitude (km)	ū (m/s)	v̄ (m/s)	s_u (m/s)	s_v (m/s)	r(u,v) (m/s)
0.	-1.6224	0.6125	2.9828	2.5915	-0.0421
1.	-0.7132	0.8957	5.2390	4.2560	0.1414
2.	0.5620	-0.3020	5.6185	4.5509	0.2933
3.	1.6107	-0.4585	5.9701	4.9028	0.2884
4.	2.7633	-0.5193	6.4756	5.4555	0.2623
5.	4.2107	-0.6553	6.8665	5.8869	0.2479
6.	5.6727	-0.8238	7.4119	6.6910	0.2275
7.	7.2656	-0.8190	8.0676	7.4957	0.2516
8.	8.8155	-0.6196	8.9158	8.5744	0.2461
9.	10.4326	-0.8036	9.7393	10.0306	0.2422
10.	12.2645	-0.9546	11.1501	11.5000	0.2682
11.	14.5611	-1.2486	12.3306	13.0673	0.2979
12.	16.8947	-1.6645	13.5083	14.2654	0.3181
13.	18.9828	-2.8242	13.9007	14.0164	0.3343
14.	18.7754	-3.1544	12.1751	12.1398	0.3679
15.	15.8735	-3.5526	9.9259	9.6692	0.4062
16.	11.8944	-3.4742	8.3151	7.5733	0.3613
17.	7.4216	-3.0999	6.8568	6.0374	0.3374
18.	3.1352	-2.5008	5.7910	4.7211	0.2553
19.	-0.2638	-1.5993	4.8257	3.6892	0.1643
20.	-2.5797	-1.2481	4.4434	3.0276	0.1617
21.	-4.4085	-0.7432	4.2570	2.6804	0.0324
22.	-5.6244	-0.6809	4.2943	2.8047	-0.0557
23.	-6.4443	-0.4819	4.3037	2.7450	-0.0322
24.	-6.9350	-0.4455	4.6712	2.8440	0.0262
25.	-7.1096	-0.6147	5.1054	2.9632	0.0070
26.	-7.1516	-0.5847	5.5478	3.0243	0.0310
27.	-6.8694	-0.6441	6.0256	3.0590	-0.0122

TABLE A-2. THE FOUR WIND VECTORS IN CARTESIAN COORDINATES FOR THE LARGEST COMPONENTS RELATIVE TO THE MONTHLY MEAN WIND TO THE 85-PERCENT PROBABILITY ELLIPSE. FLIGHT AZIMUTH OF 90°, MAY.KSC

Altitude (km)	x_1 (m/s)	y_1 (m/s)	x_2 (m/s)	y_2 (m/s)	x_3 (m/s)	y_3 (m/s)	x_4 (m/s)	y_4 (m/s)
0.	4.2	0.4	-1.9	5.7	-7.4	0.8	-1.4	-4.4
1.	9.5	2.1	0.7	9.2	-10.9	-0.3	-2.2	-7.4
2.	11.5	2.3	3.8	8.6	-10.4	-2.9	-2.6	-9.2
3.	13.2	2.3	5.0	9.1	-10.0	-3.2	-1.7	-10.0
4.	15.4	2.3	6.1	10.1	-9.9	-3.3	-0.5	-11.1
5.	17.6	2.2	7.5	10.8	-9.2	-3.5	0.9	-12.1
6.	20.1	2.1	9.0	12.2	-8.8	-3.8	2.4	-13.9
7.	23.0	2.9	11.2	13.8	-8.4	-4.5	3.3	-15.4
8.	26.2	3.5	13.1	16.1	-8.6	-4.7	4.5	-17.3
9.	29.4	3.9	15.0	18.7	-8.5	-5.5	5.8	-20.3
10.	34.0	5.1	18.1	21.4	-9.5	-7.0	6.4	-23.4
11.	38.6	6.3	21.7	24.2	-9.5	-8.8	7.4	-26.7
12.	43.2	7.2	25.3	26.1	-9.4	-10.5	8.5	-29.5
13.	46.1	6.3	28.0	24.5	-8.1	-12.0	9.9	-30.1
14.	42.5	5.5	27.5	20.5	-4.9	-11.9	10.1	-26.8
15.	35.2	4.1	23.7	15.3	-3.5	-11.2	8.0	-22.4
16.	28.1	1.9	17.7	11.3	-4.3	-8.8	6.0	-18.2
17.	20.8	0.9	11.9	8.7	-5.9	-7.1	2.9	-14.9
18.	14.4	-0.2	6.0	6.7	-8.1	-4.8	0.3	-11.7
19.	9.1	-0.4	1.3	5.6	-9.7	-2.8	-1.8	-8.8
20.	6.1	-0.3	-1.2	4.6	-11.2	-2.2	-4.0	-7.1
21.	3.9	-0.6	-4.1	4.5	-12.7	-0.9	-4.7	-6.0
22.	2.7	-1.0	-6.1	4.8	-14.0	-0.4	-5.2	-6.1
23.	1.9	-0.7	-6.7	4.9	-14.8	-0.3	-6.2	-5.8
24.	2.2	-0.3	-6.7	5.1	-16.0	-0.6	-7.2	-6.0
25.	2.8	-0.6	-7.0	5.2	-17.1	-0.7	-7.2	-6.4
26.	3.7	-0.4	-6.8	5.3	-18.0	-0.8	-7.5	-6.5
27.	4.9	-0.7	-7.0	5.3	-18.6	-0.6	-6.7	-6.6

TABLE A-3. THE FOUR WIND VECTORS IN POLAR COORDINATES FOR THE LARGEST COMPONENTS RELATIVE TO THE MONTHLY MEAN WIND TO THE 85-PERCENT PROBABILITY ELLIPSE, FLIGHT AZIMUTH OF 90°, MAY, KSC

Altitude (km)	W_1 (m/s)	θ_1 (deg)	W_2 (m/s)	θ_2 (deg)	W_3 (m/s)	θ_3 (deg)	W_4 (m/s)	θ_4 (deg)	Monthly Mean W_R (m/s)	Monthly Mean θ_R (deg)
0.	4.2	264.5	6.0	161.7	7.5	96.3	4.6	17.3	1.73	110.68
1.	9.7	257.7	9.2	184.5	10.9	88.5	7.7	16.3	1.14	141.47
2.	11.7	258.7	9.4	203.8	10.8	74.4	9.5	16.1	0.64	298.25
3.	13.4	260.2	10.4	208.6	10.5	72.2	10.2	9.9	1.67	285.89
4.	15.5	261.6	11.8	211.0	10.4	71.4	11.2	2.8	2.81	280.64
5.	17.7	262.9	13.2	214.8	9.8	69.1	12.2	355.8	4.26	278.85
6.	20.2	263.9	15.1	216.3	9.5	66.6	14.1	350.2	5.73	278.26
7.	23.2	262.9	17.8	219.1	9.6	62.0	15.8	347.9	7.31	276.43
8.	26.4	262.4	20.7	219.1	9.8	61.1	17.9	345.3	8.84	274.02
9.	29.7	262.4	24.0	218.7	10.2	57.0	21.2	344.0	10.46	274.40
10.	34.4	261.5	28.1	220.1	11.7	53.6	24.2	344.6	12.30	274.45
11.	39.1	260.7	32.5	221.9	12.9	47.0	27.7	344.5	14.61	274.90
12.	43.8	260.6	36.3	224.0	14.1	41.9	30.7	343.9	16.98	275.63
13.	46.5	262.2	37.2	228.9	14.4	34.1	31.7	341.8	19.19	278.46
14.	42.9	262.6	34.3	233.3	12.8	22.6	28.6	339.4	19.04	279.54
15.	35.4	263.4	28.2	237.2	11.7	17.2	23.8	340.3	16.27	282.62
16.	28.2	266.2	21.0	237.6	9.8	26.0	19.2	341.7	12.39	286.28
17.	20.8	267.6	14.7	234.0	9.2	40.0	15.1	348.9	8.04	292.67
18.	14.4	270.6	9.0	221.9	9.5	59.2	11.7	358.7	4.01	308.58
19.	9.1	272.6	5.7	192.9	10.1	74.0	9.0	11.6	1.62	9.37
20.	6.1	272.8	4.8	165.8	11.4	78.9	8.2	29.1	2.87	64.18
21.	3.9	278.4	6.1	137.2	12.7	85.9	7.6	38.1	4.47	80.43
22.	2.9	289.8	7.7	128.1	14.0	88.5	8.0	40.0	5.67	83.10
23.	2.0	288.6	8.3	125.9	14.8	88.8	8.5	46.6	6.46	85.72
24.	2.2	277.9	8.4	127.3	16.0	87.9	9.3	50.2	6.95	86.32
25.	2.9	281.5	8.7	126.2	17.1	87.8	9.6	48.3	7.14	85.06
26.	3.7	276.3	8.6	127.9	18.0	87.6	9.9	49.1	7.18	85.33
27.	4.9	278.4	8.8	127.2	18.6	88.2	9.4	45.5	6.90	84.64

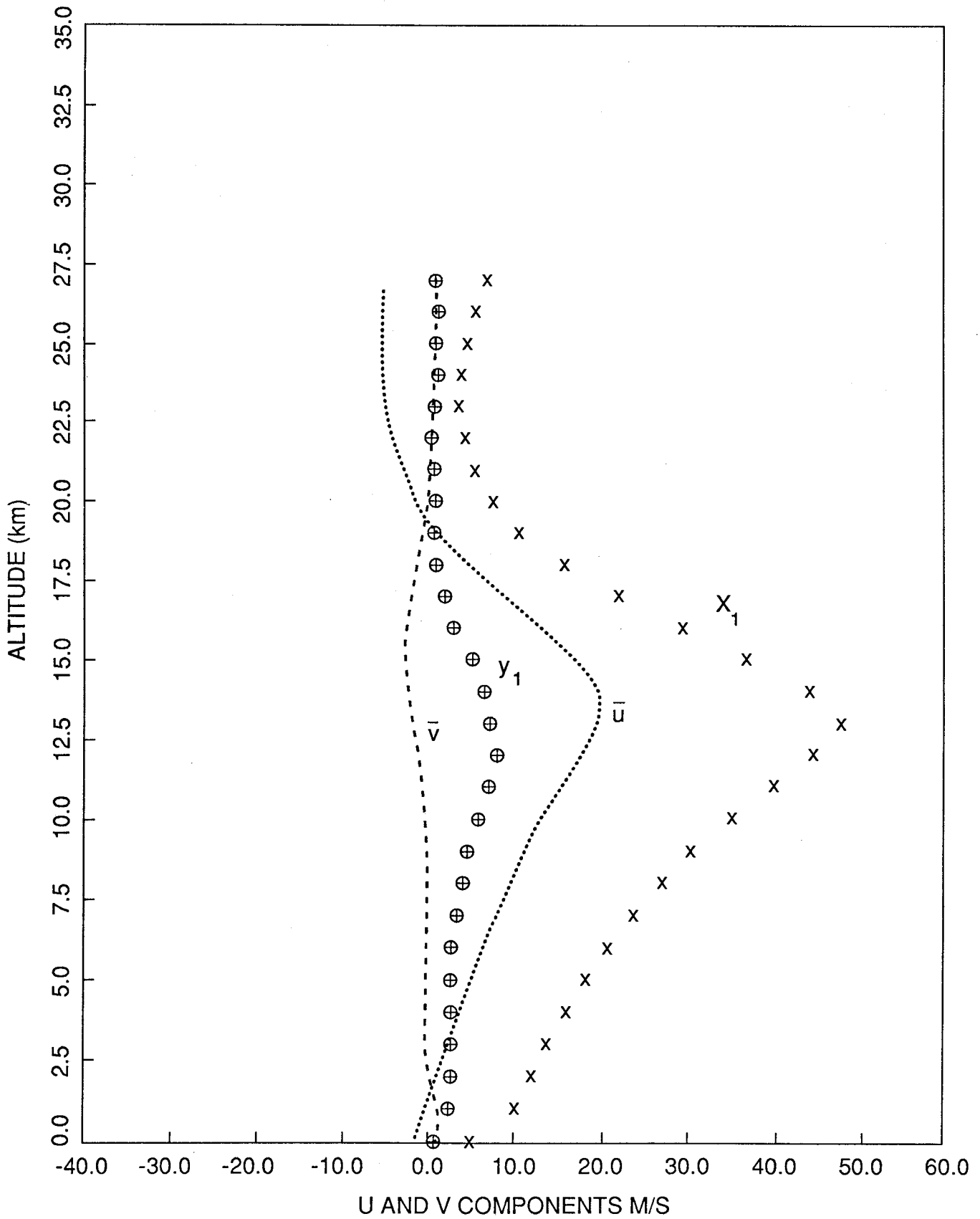W is windspeed, θ is wind direction, meteorological coordinates.

Figure A-1. Wind vector profile components for largest tail wind component relative to the monthly mean wind to the 85-percent ellipse, flight azimuth of 90°, May, KSC.
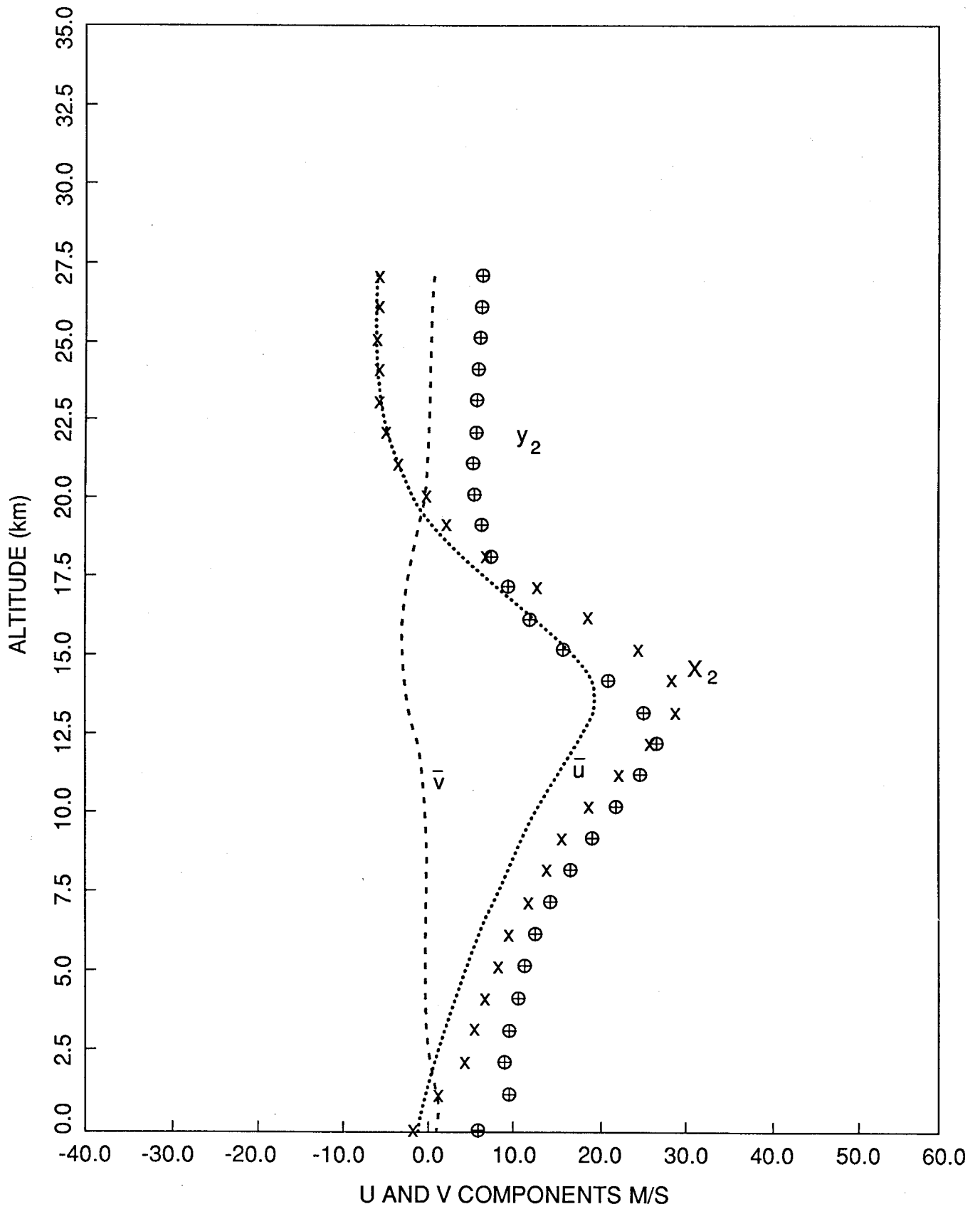
Figure A-2. Wind vector profile components for largest right to left crosswind component
relative to the monthly mean wind to the 85-percent ellipse, flight azimuth
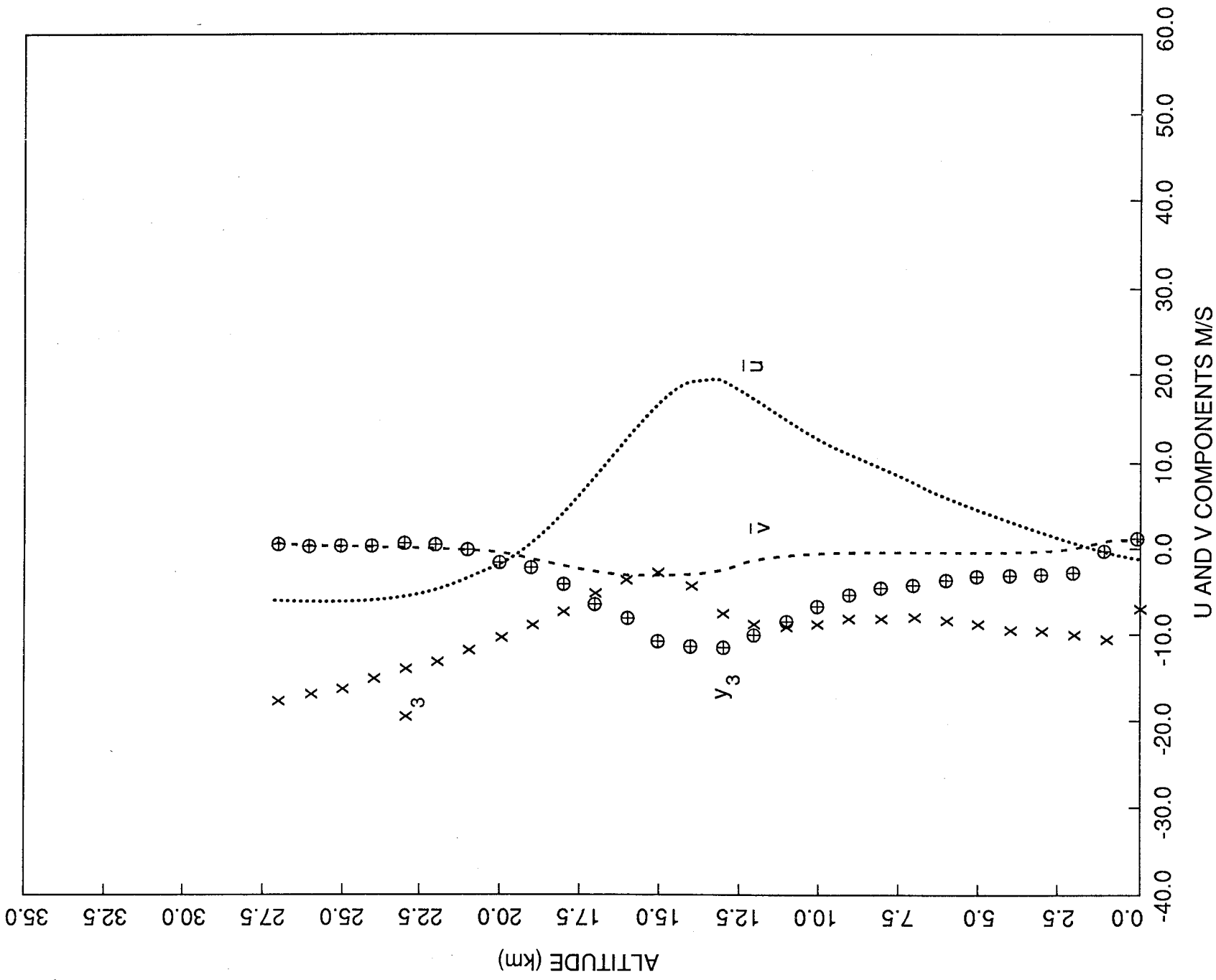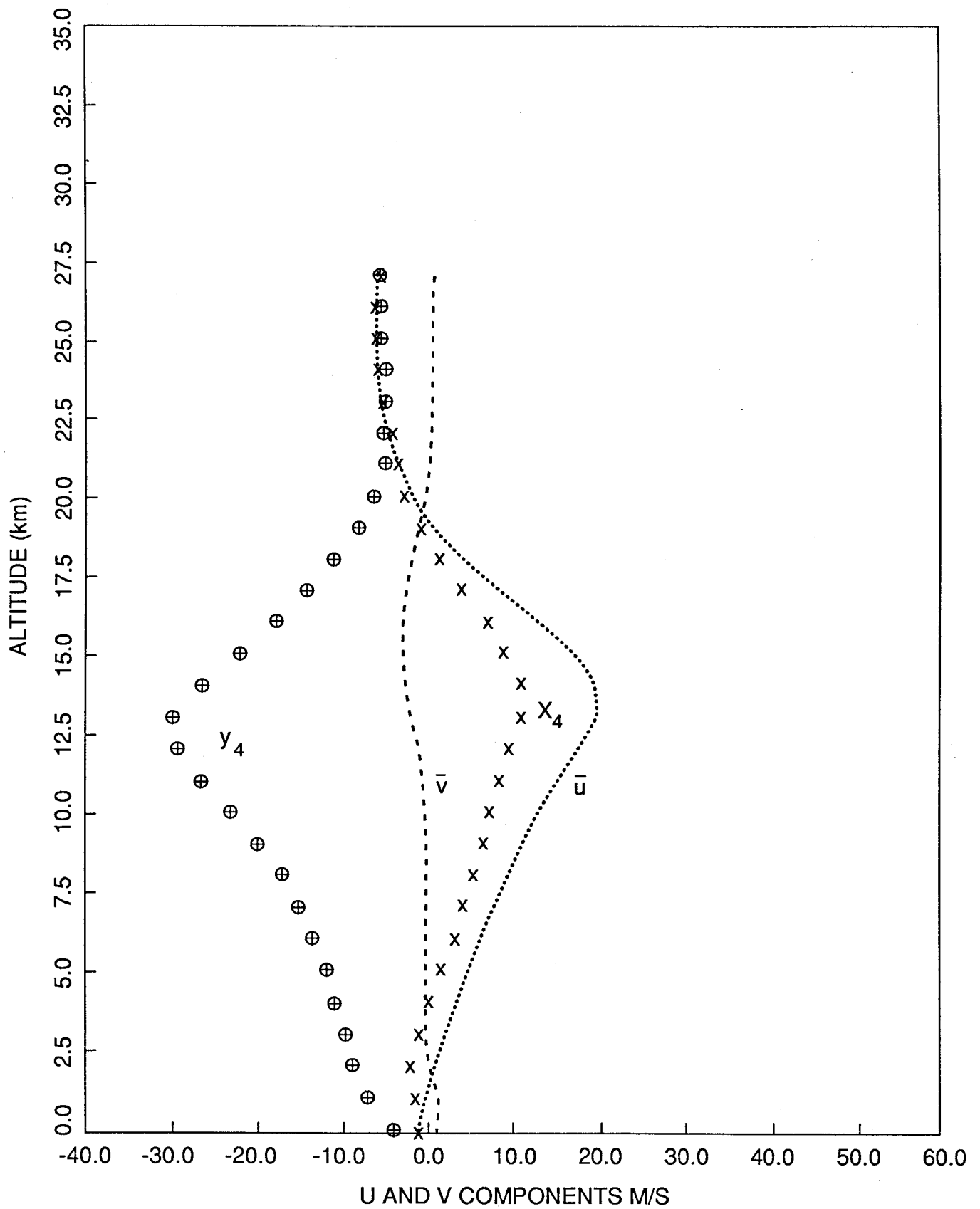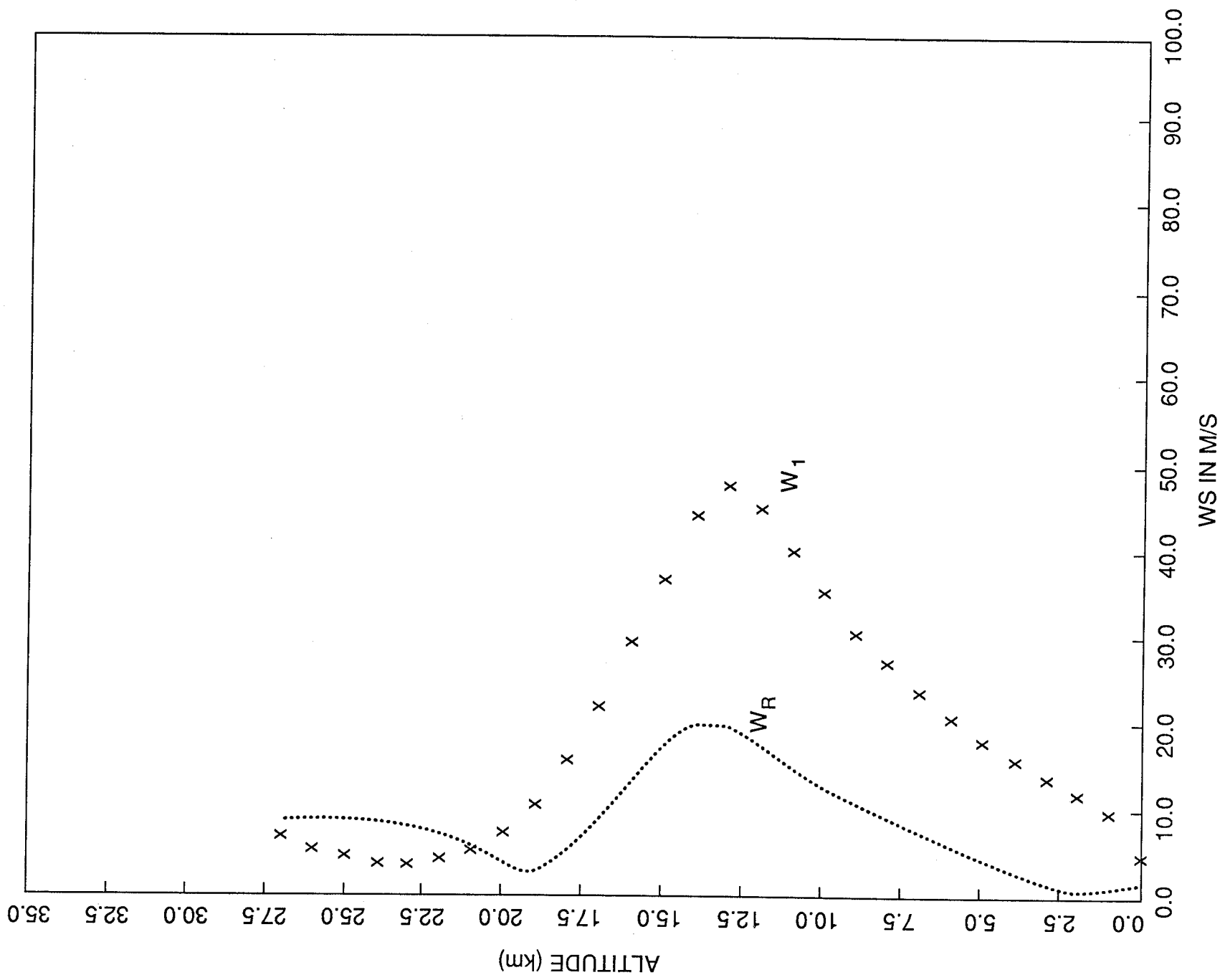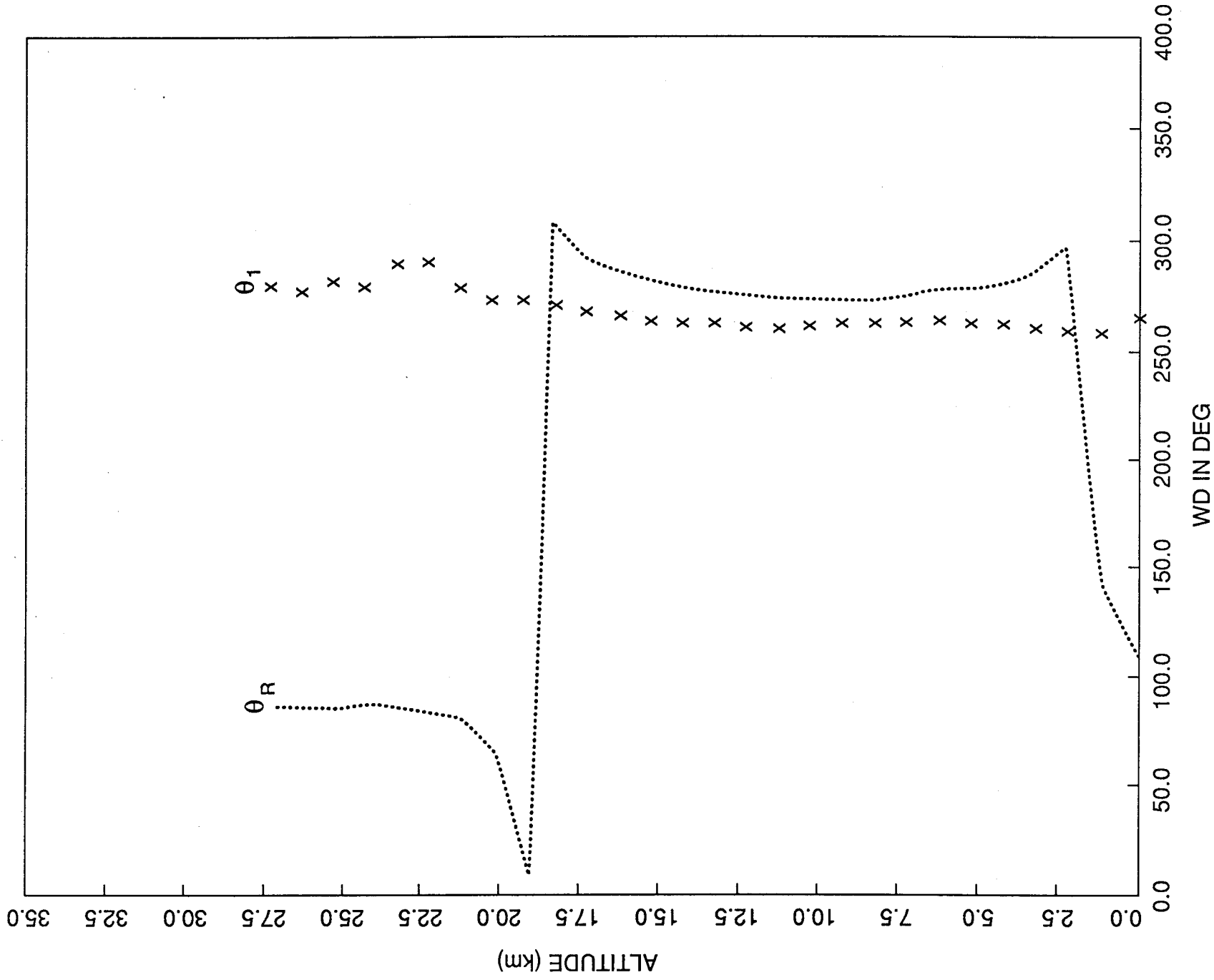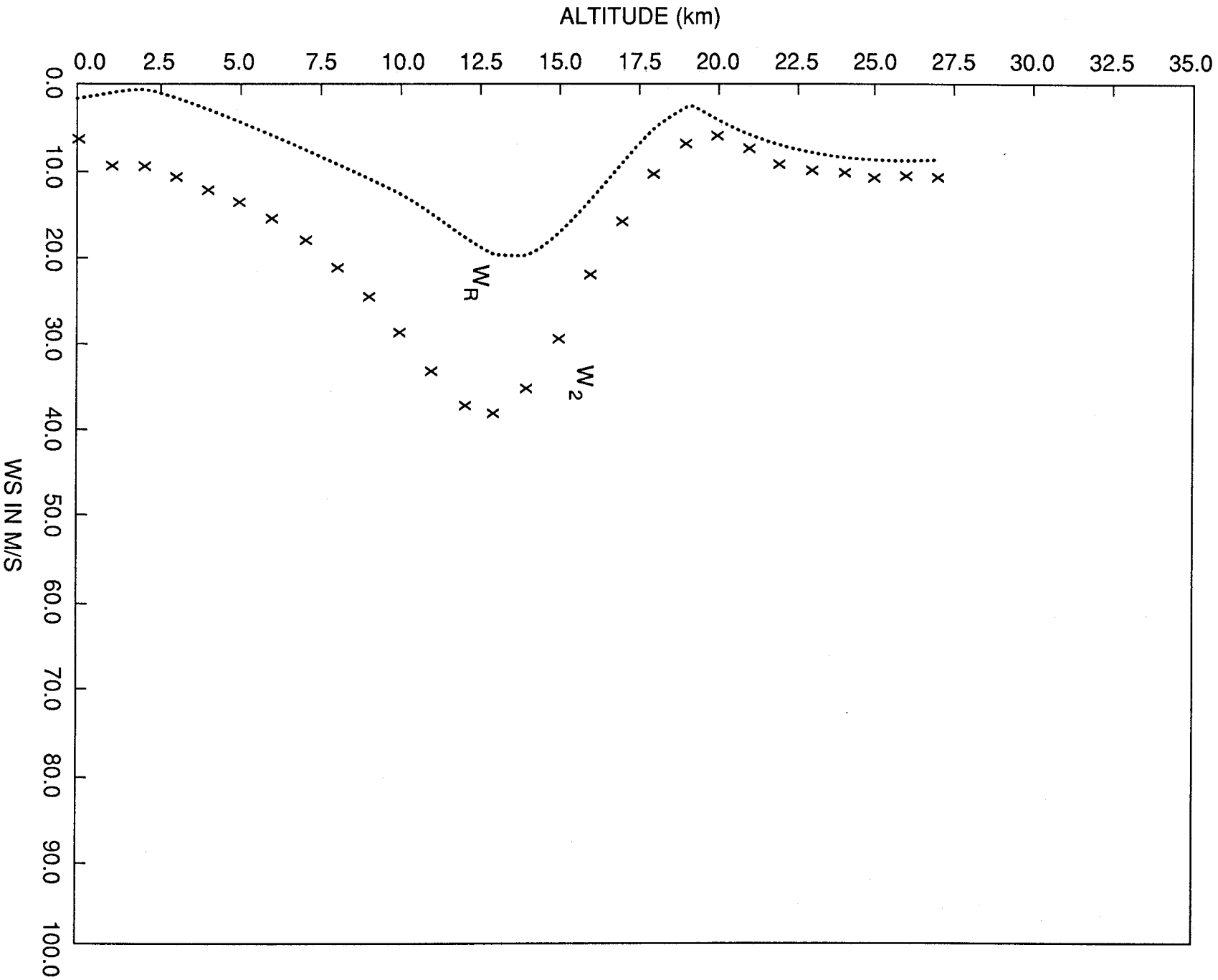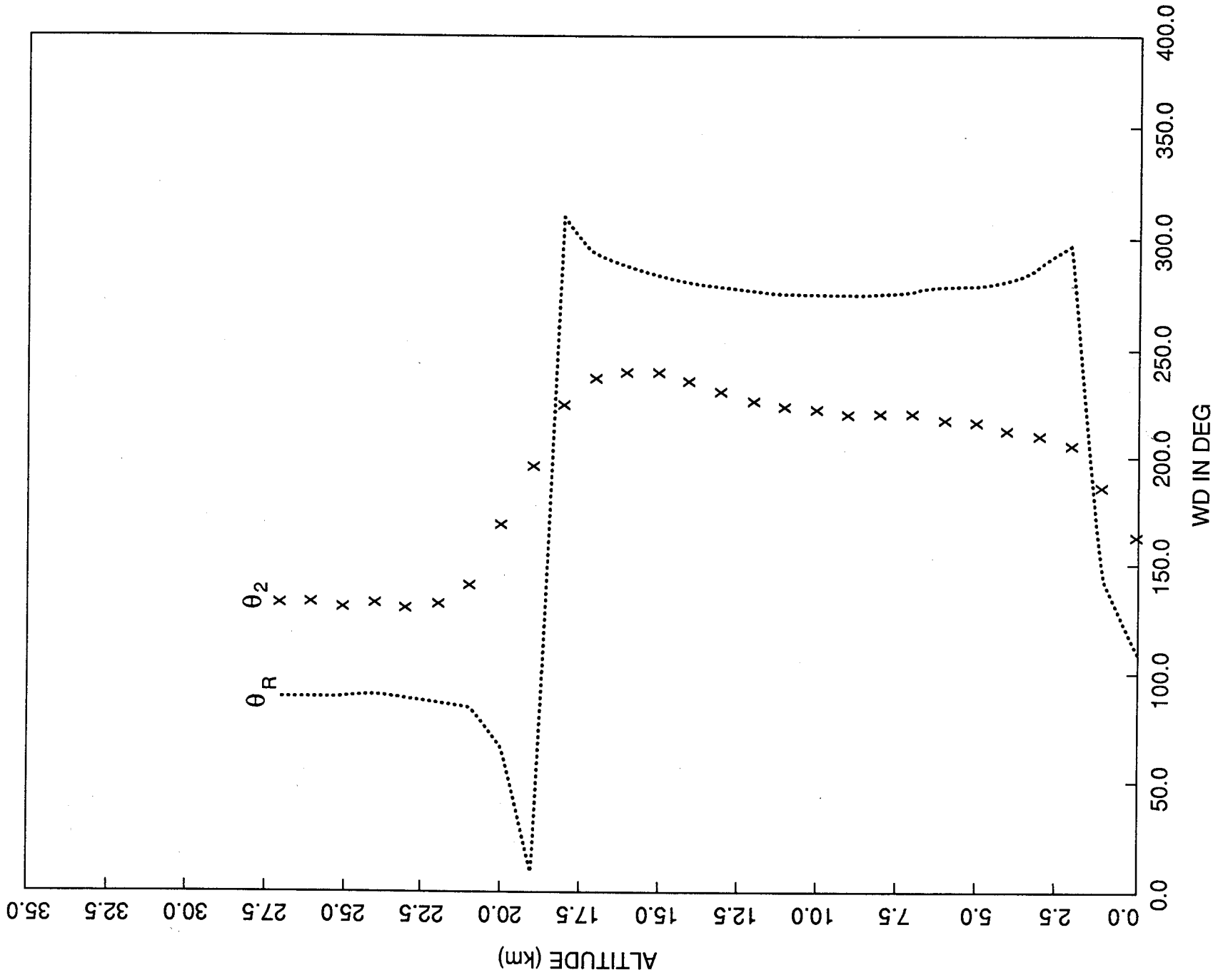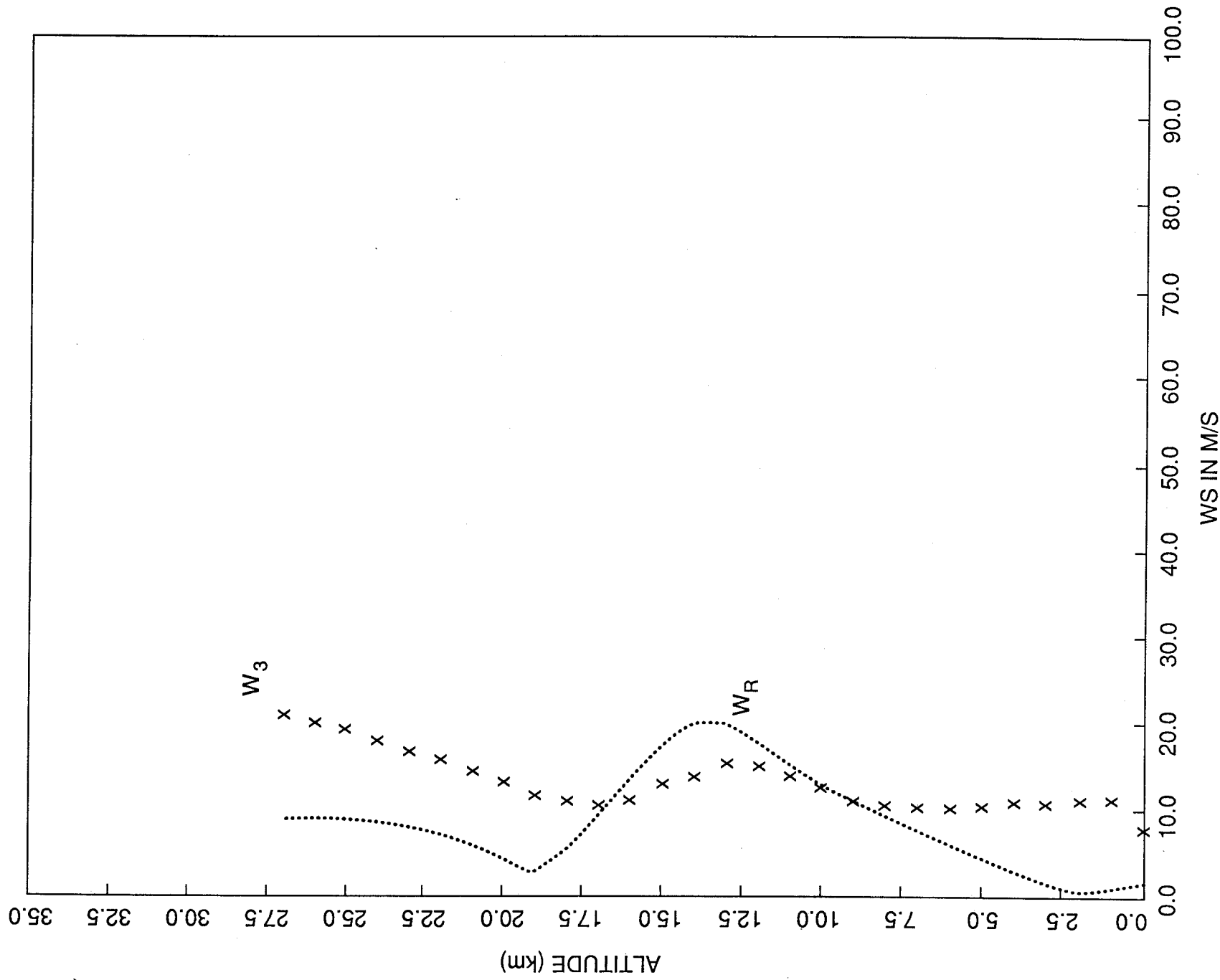of 90°, May, KSC.

Figure A-3. Wind vector profile components for largest head wind component relative to the monthly mean wind to the 85-percent ellipse, flight azimuth of 90°, May, KSC.

Figure A-4. Wind vector profile components for largest left to right wind component relative to the monthly mean wind to the 85-percent ellipse, flight azimuth of 90°, May, KSC.

Figure A-5. Wind speed for the largest tail wind component relative to the monthly mean wind to the 85-percent ellipse, flight azimuth of 90°, May, KSC.
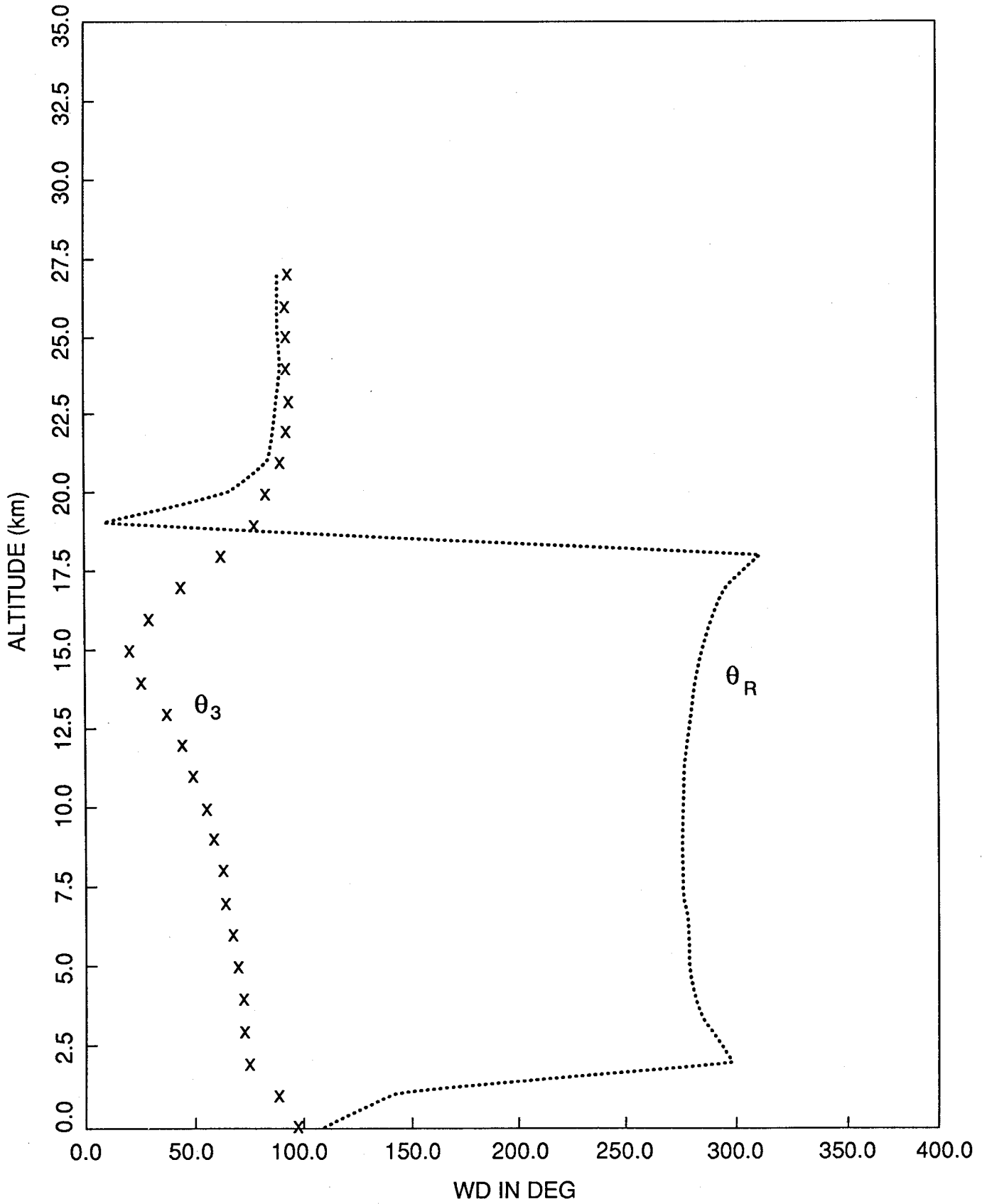
Figure A-6. Wind direction for the largest tail wind component relative to the monthly mean wind to the 85-percent ellipse. flight azimuth of 90°. May. KSC.
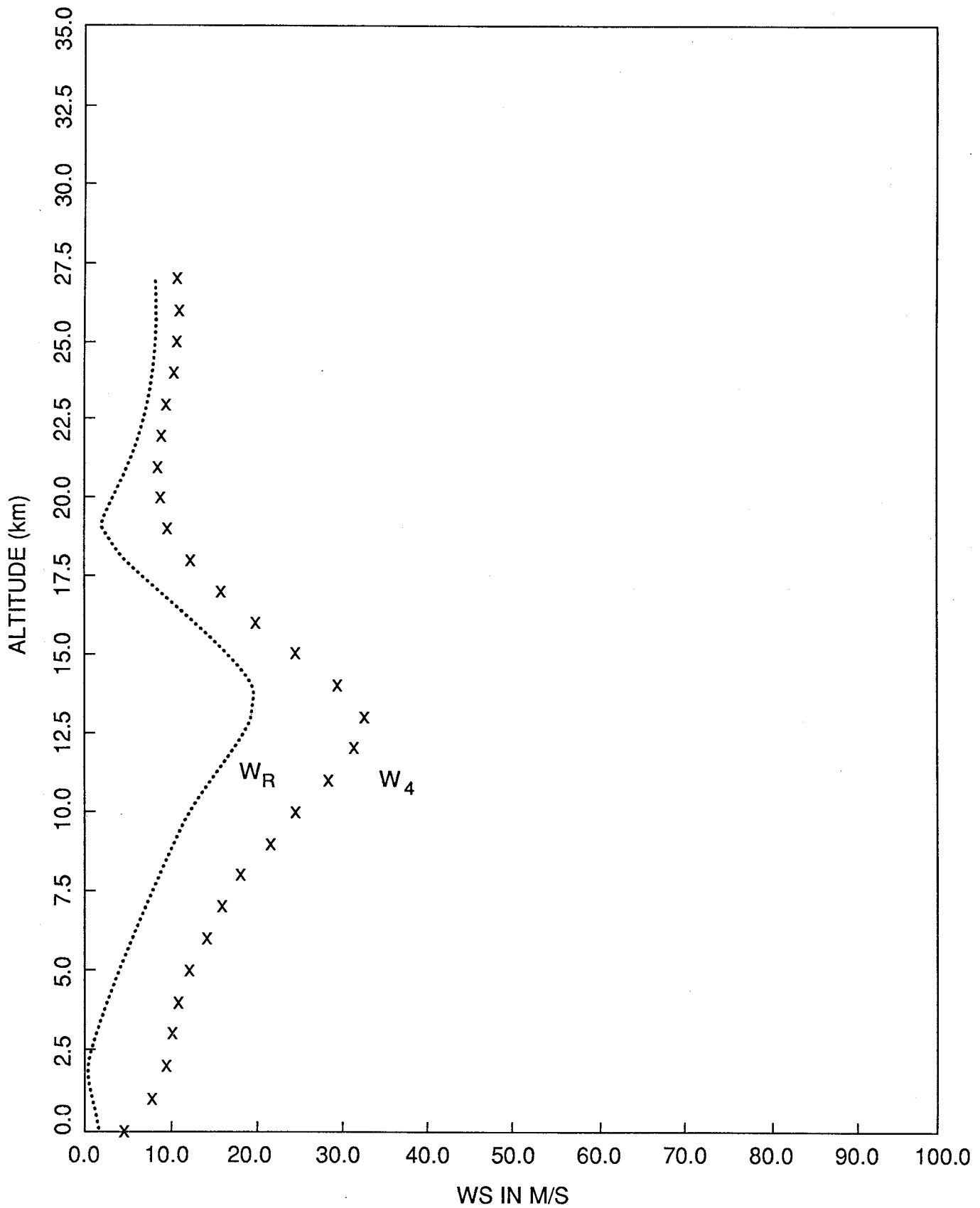
31

Figure A-7. Wind speed for the largest right to left cross wind component relative to the monthly mean wind to the 85-percent ellipse, flight azimuth of 90°, May, KSC.
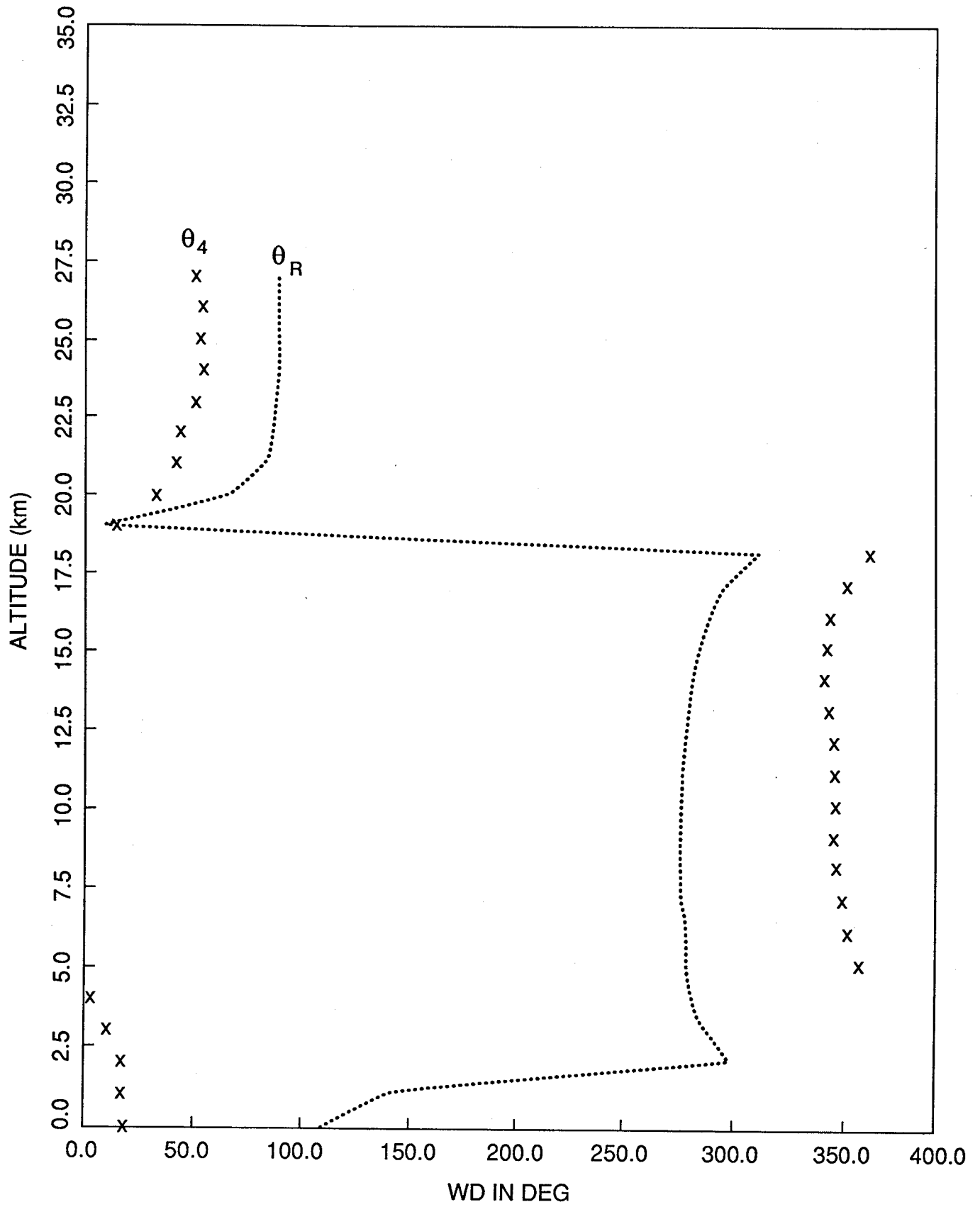
Figure A-8. Wind direction for the largest right to left wind component relative to the monthly mean wind to the 85-percent ellipse, flight azimuth of 90°, May, KSC.

Figure A-9. Wind speed for the largest head wind component relative to the monthly mean wind to the 85-percent ellipse, flight azimuth of 90°, May, KSC.

Figure A-10. Wind direction for the largest head wind component relative to the monthly mean wind to the 85-percent ellipse, flight azimuth of 90°, May, KSC.

Figure A-11. Wind speed for the largest left to right cross wind component relative to the monthly mean wind to the 85-percent ellipse, flight azimuth of 90°, May, KSC.

Figure A-12. Wind direction for the largest left to right cross wind component relative to the monthly mean wind to the 85 percent ellipse, flight azimuth of 90°, May, KSC.

APPENDIX B

TABLE B-1. FOUR WIND VECTORS IN CARTESIAN COORDINATES TO THE SEMI-MAJOR AND SEMI-MINOR AXES TO THE 85-PERCENT PROBABILITY ELLIPSE, FLIGHT OF 90°, MAY, KSC

Altitude	U1	V1	U2	V2	U3	V3	U4	V4
0.	4.1	-0.2	-0.9	5.6	-7.4	1.5	-2.3	-4.4
1.	9.2	3.9	-3.1	8.6	-10.6	-2.1	1.6	-6.8
2.	10.9	5.0	-3.1	6.8	-9.8	-5.6	4.2	-7.4
3.	12.5	5.3	-2.4	7.2	-9.3	-6.2	5.6	-8.1
4.	14.5	5.8	-1.8	8.0	-9.0	-6.9	7.4	-9.0
5.	16.6	6.2	-0.9	8.5	-8.2	-7.5	9.3	-9.8
6.	18.6	7.5	-0.8	9.2	-7.2	-9.2	12.1	-10.8
7.	20.9	9.4	-0.6	9.6	-6.4	-11.0	15.1	-11.3
8.	23.3	11.7	-0.8	10.6	-5.7	-13.0	18.4	-11.8
9.	26.5	13.4	-0.7	11.7	-5.6	-15.0	21.5	-13.3
10.	30.8	15.6	-0.3	13.1	-6.3	-17.5	24.8	-15.0
11.	36.4	16.7	1.4	14.7	-7.2	-19.2	27.7	-17.2
12.	40.7	18.4	2.5	15.4	-6.9	-21.7	31.3	-18.7
13.	41.5	19.1	3.5	13.1	-3.5	-24.8	34.5	-18.7
14.	38.4	16.4	5.5	10.2	-0.9	-22.7	32.0	-16.5
15.	32.4	11.9	5.8	7.2	-0.6	-19.0	25.9	-14.3
16.	26.2	7.6	4.4	6.2	-2.5	-14.6	19.4	-13.2
17.	19.5	5.2	1.7	5.2	-4.6	-11.4	13.2	-11.4
18.	13.8	2.6	-0.5	5.1	-7.5	-7.6	6.8	-10.1
19.	8.9	1.0	-2.1	5.1	-9.5	-4.2	1.6	-8.3
20.	6.0	0.4	-3.7	4.4	-11.2	-2.9	-1.5	-6.9
21.	3.9	-0.5	-4.6	4.5	-12.7	-1.0	-4.2	-6.0
22.	2.7	-1.2	-5.3	4.8	-14.0	-0.2	-6.0	-6.1
23.	1.9	-0.8	-6.3	4.9	-14.8	-0.2	-6.6	-5.8
24.	2.2	-0.2	-7.1	5.1	-16.0	-0.7	-6.8	-6.0
25.	2.8	-0.6	-7.1	5.2	-17.1	-0.7	-7.1	-6.4
26.	3.7	-0.3	-7.3	5.3	-18.0	-0.8	-7.0	-6.5
27.	4.9	-0.7	-6.8	5.3	-18.6	-0.5	-6.9	-6.6

Units: Components – m/s, altitude – km.

TABLE B-2. FOUR WIND VECTORS IN POLAR COORDINATES TO THE SEMI-MAJOR
AND SEMI-MINOR AXES TO THE 85-PERCENT PROBABILITY ELLIPSE,
FLIGHT AZIMUTH 90°, MAY, KSC

Altitude	WS1	WD1	WS2	WD2	WS3	WD3	WS4	WD4
0.	4.1	273.2	5.7	170.9	7.5	101.1	5.0	28.3
1.	10.0	246.9	9.1	160.3	10.9	78.6	7.0	346.4
2.	12.0	245.5	7.5	155.7	11.2	60.3	8.5	330.5
3.	13.6	247.1	7.6	161.5	11.2	56.3	9.9	325.2
4.	15.6	248.1	8.2	167.1	11.3	52.6	11.7	320.9
5.	17.7	249.5	8.6	174.1	11.1	47.3	13.5	316.6
6.	20.0	248.0	9.2	175.0	11.7	38.3	16.3	311.7
7.	22.9	245.8	9.6	176.7	12.7	30.0	18.8	306.7
8.	26.1	243.2	10.6	175.8	14.2	23.6	21.9	302.8
9.	29.7	243.1	11.8	176.7	16.1	20.6	25.3	301.8
10.	34.5	243.2	13.1	178.8	18.6	19.8	29.0	301.2
11.	40.0	245.3	14.8	185.5	20.5	20.7	32.6	301.8
12.	44.6	245.7	15.6	189.4	22.8	17.6	36.4	300.9
13.	45.7	245.3	13.5	195.0	25.0	8.0	39.2	298.5
14.	41.8	247.0	11.6	208.4	22.7	2.2	36.0	297.3
15.	34.5	249.8	9.2	219.1	19.0	1.9	29.6	298.8
16.	27.3	253.8	7.6	215.1	14.8	9.6	23.5	304.2
17.	20.2	255.0	5.5	198.0	12.3	22.1	17.4	310.9
18.	14.0	259.3	5.2	174.2	10.7	44.7	12.2	326.2
19.	9.0	263.8	5.5	157.3	10.4	66.3	8.5	349.1
20.	6.0	265.7	5.7	140.0	11.5	75.2	7.0	12.0
21.	3.9	276.8	6.4	134.3	12.7	85.4	7.3	35.4
22.	3.0	293.9	7.1	132.0	14.0	89.4	8.5	44.3
23.	2.1	291.7	7.9	127.8	14.8	89.3	8.8	48.7
24.	2.2	275.7	8.7	125.7	16.0	87.6	9.1	48.6
25.	2.9	281.1	8.8	125.8	17.1	87.7	9.5	47.9
26.	3.7	275.1	9.0	126.0	18.0	87.3	9.5	47.3
27.	4.9	278.7	8.6	127.9	18.6	88.3	9.6	46.3

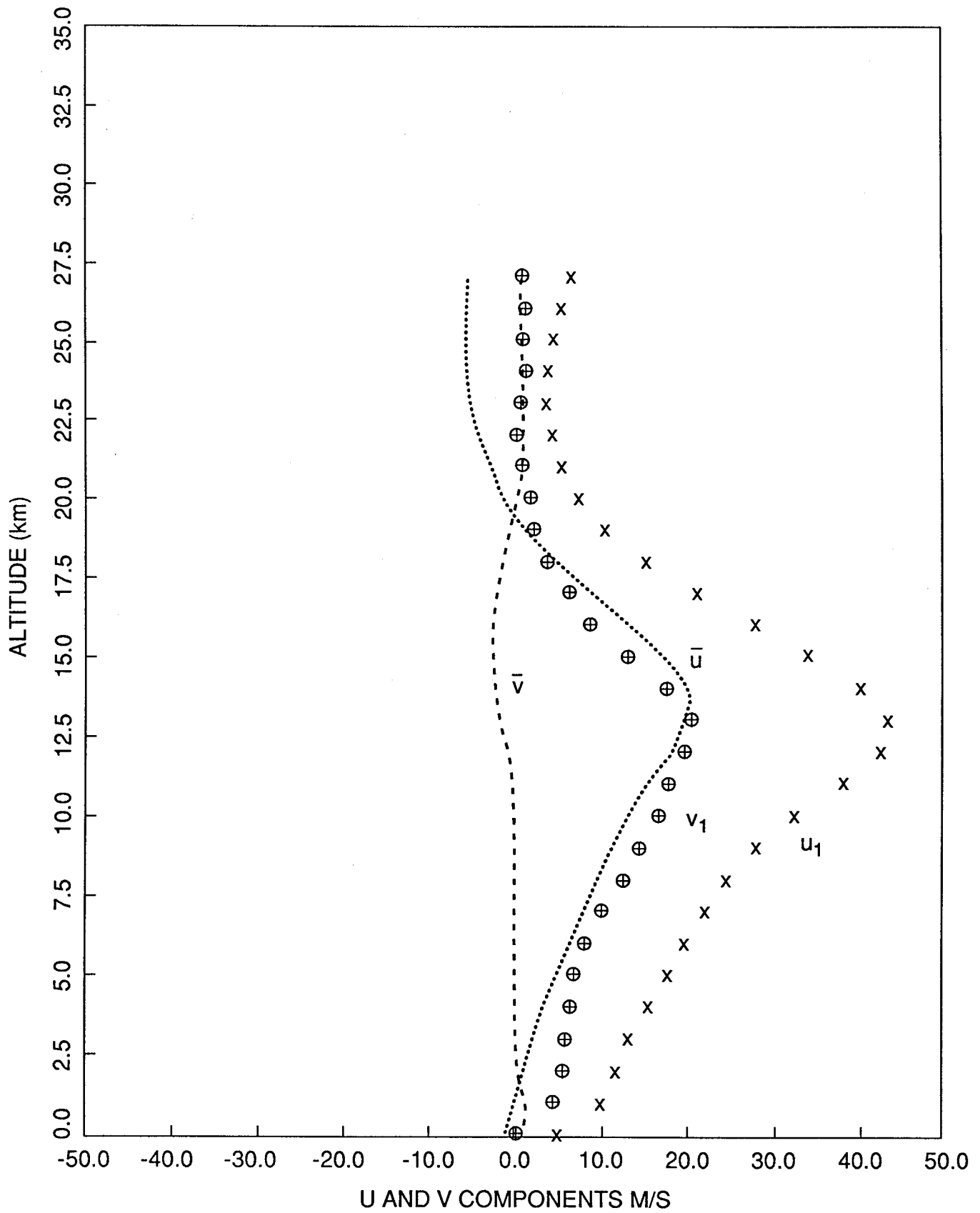Units: Wind speed – m/s; wind direction – degrees; altitude – km.

Figure B-1. Wind vector profile components to the first semi-major axis to the 85-percent probability ellipse, flight azimuth of 90°, May, KSC.
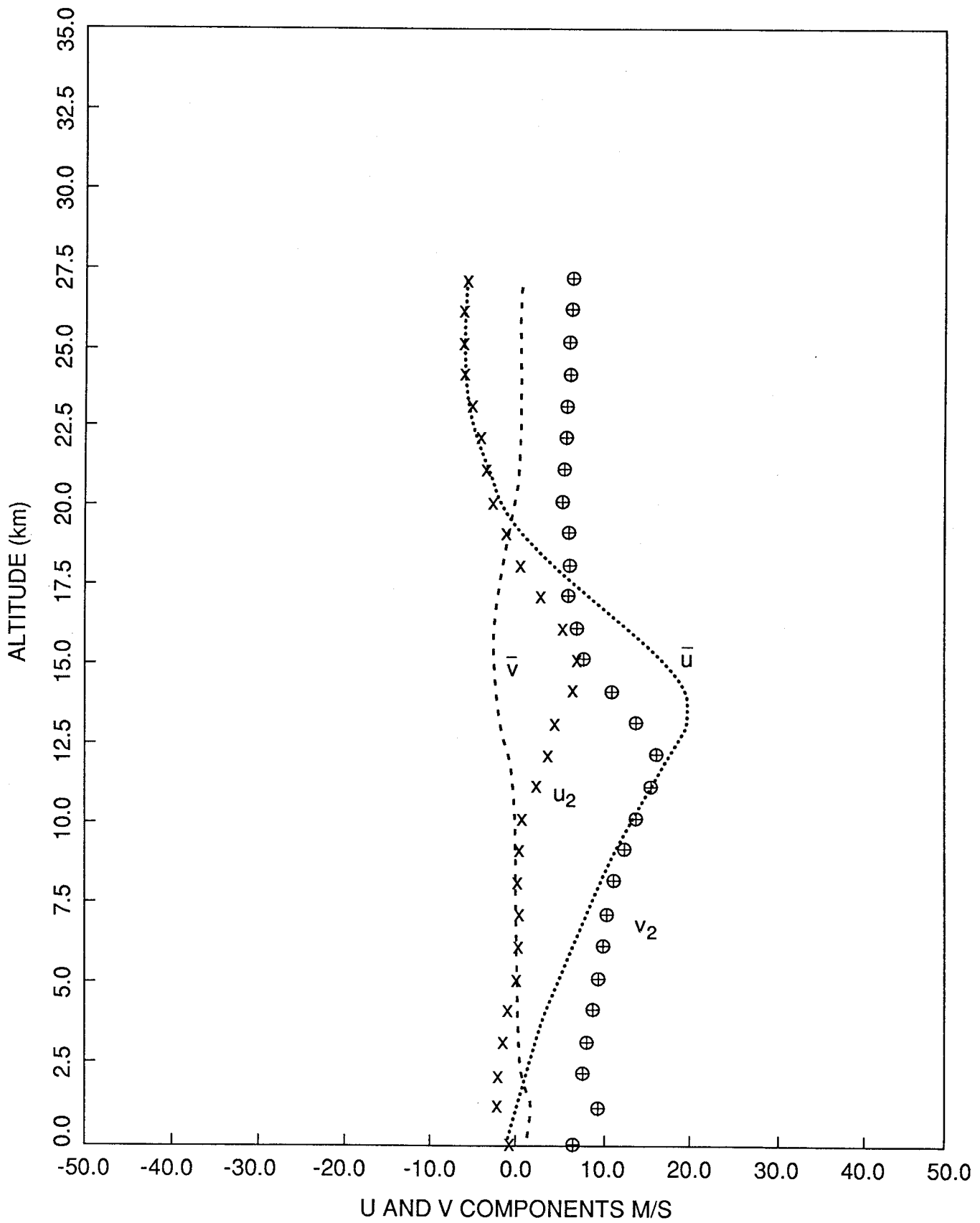
Figure B-2. Wind vector profile components to the first semi-minor axis to the 85-percent probability ellipse, flight azimuth of 90°, May, KSC.
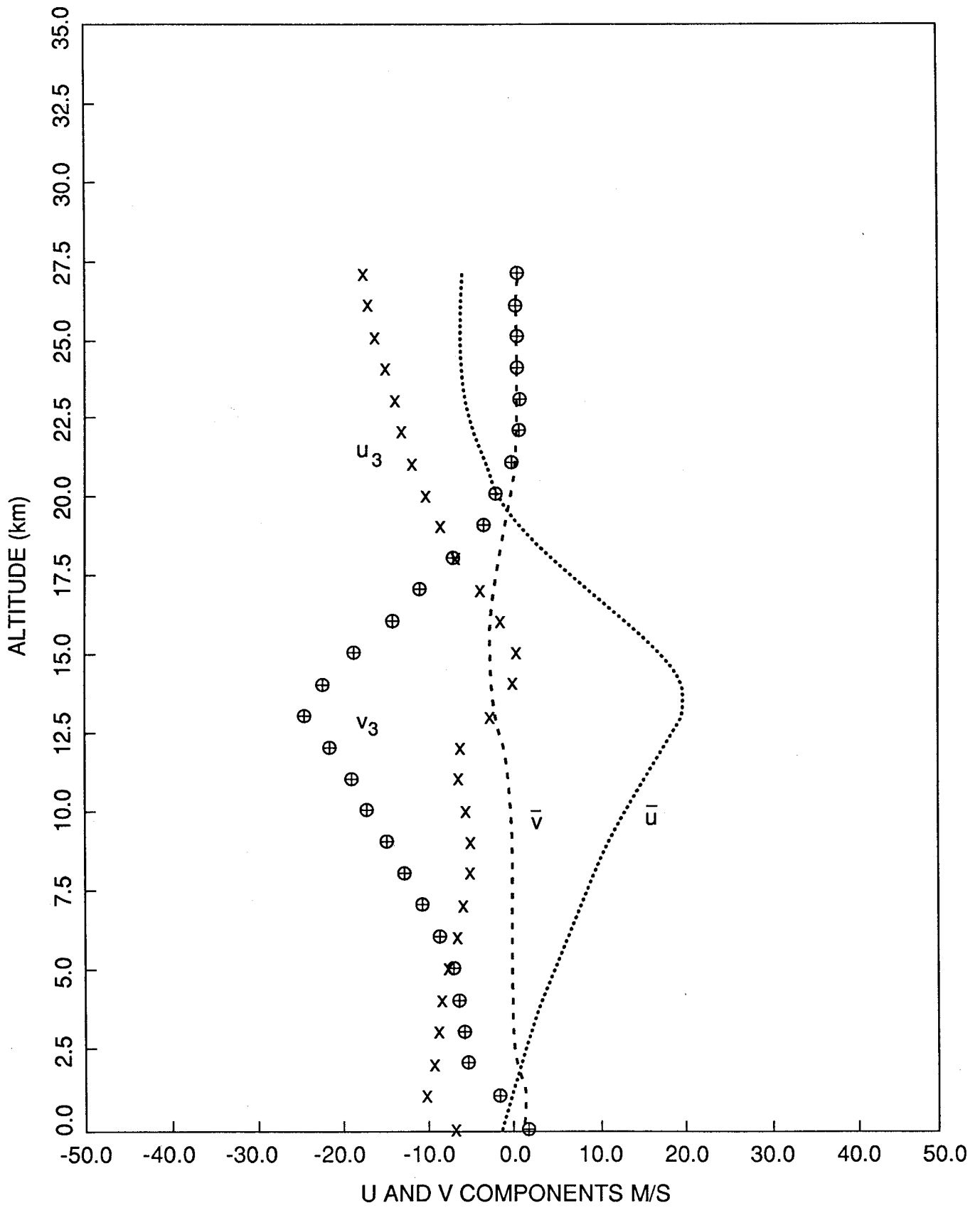
Figure B-3. Wind vector profile components to the second semi-major axis to the
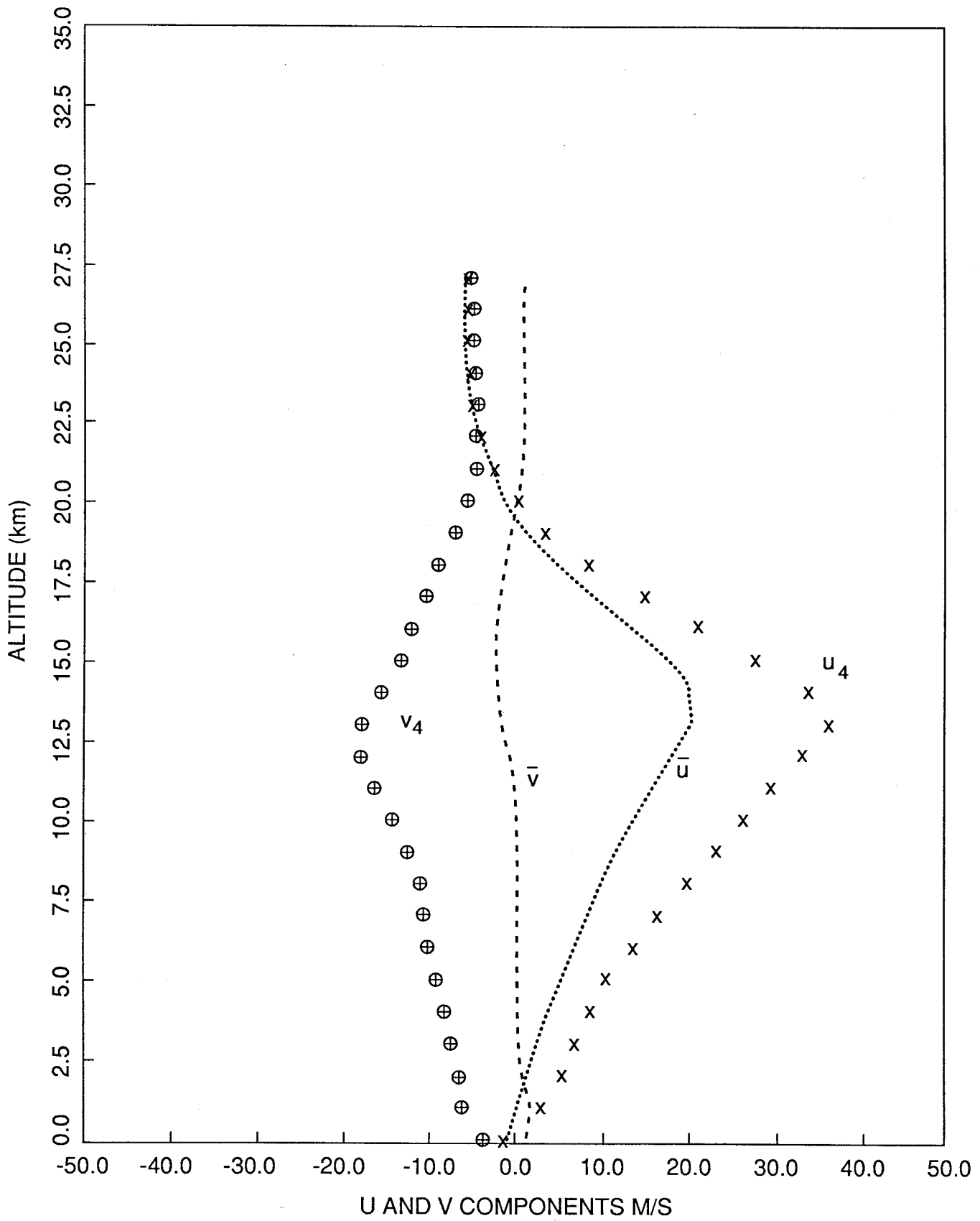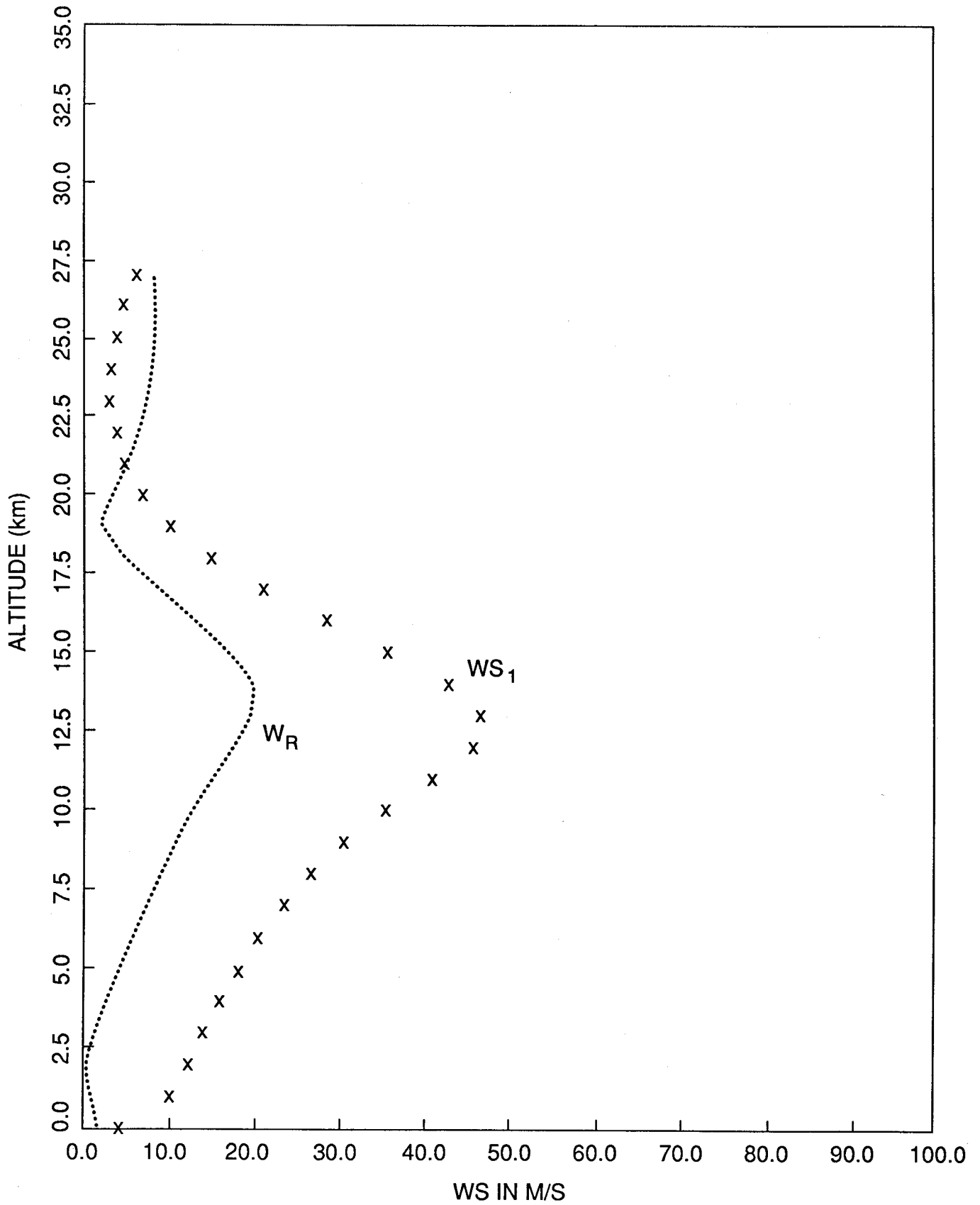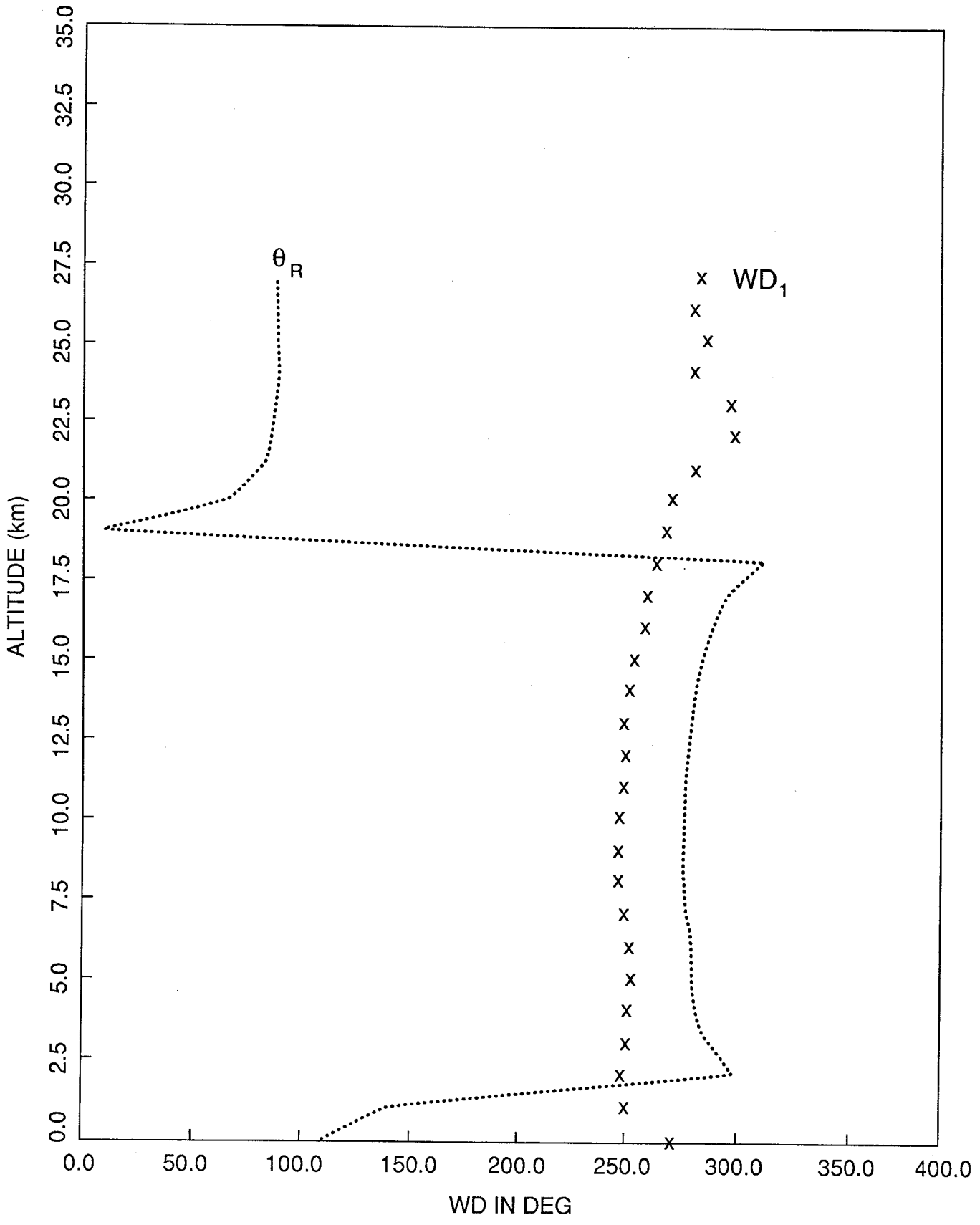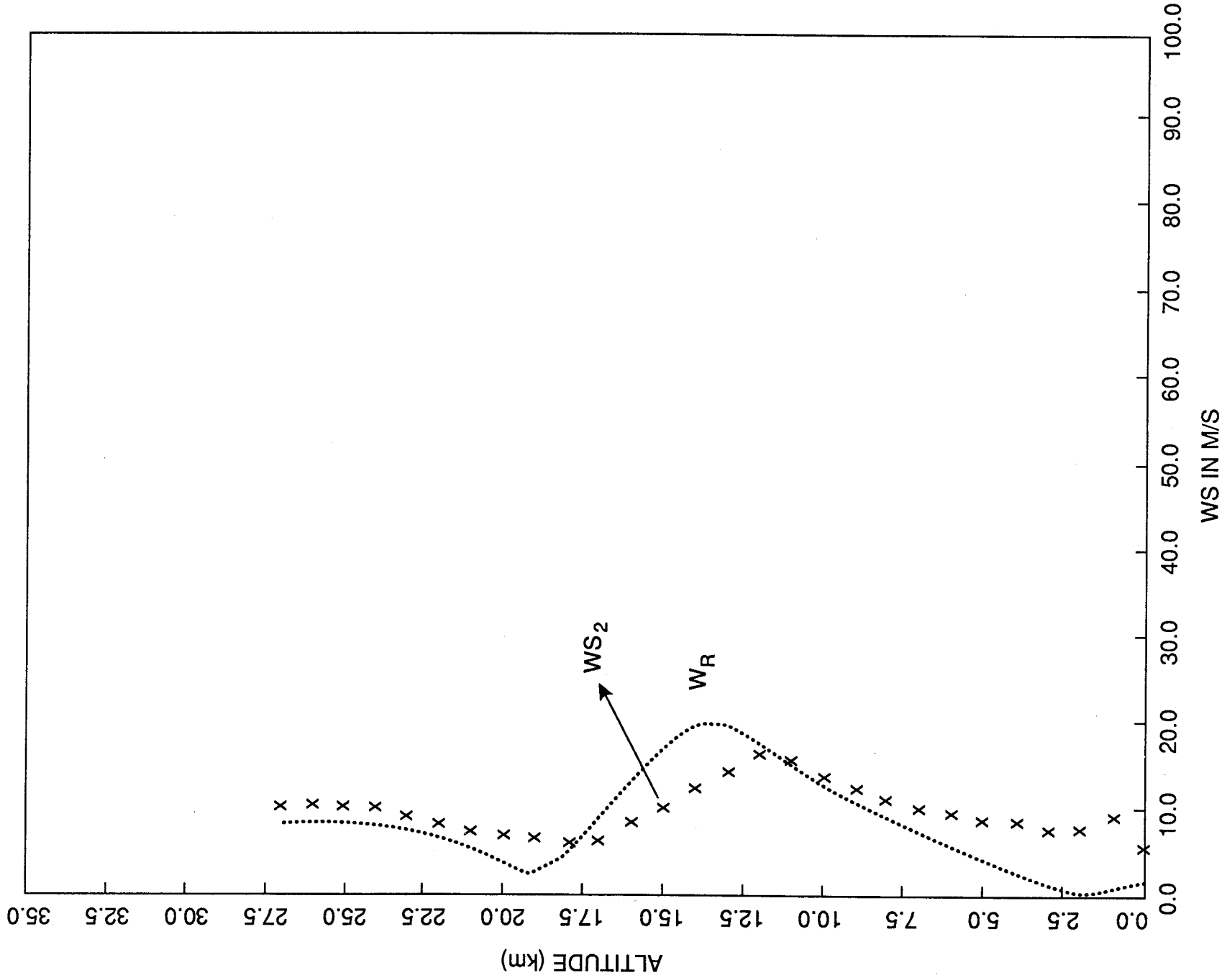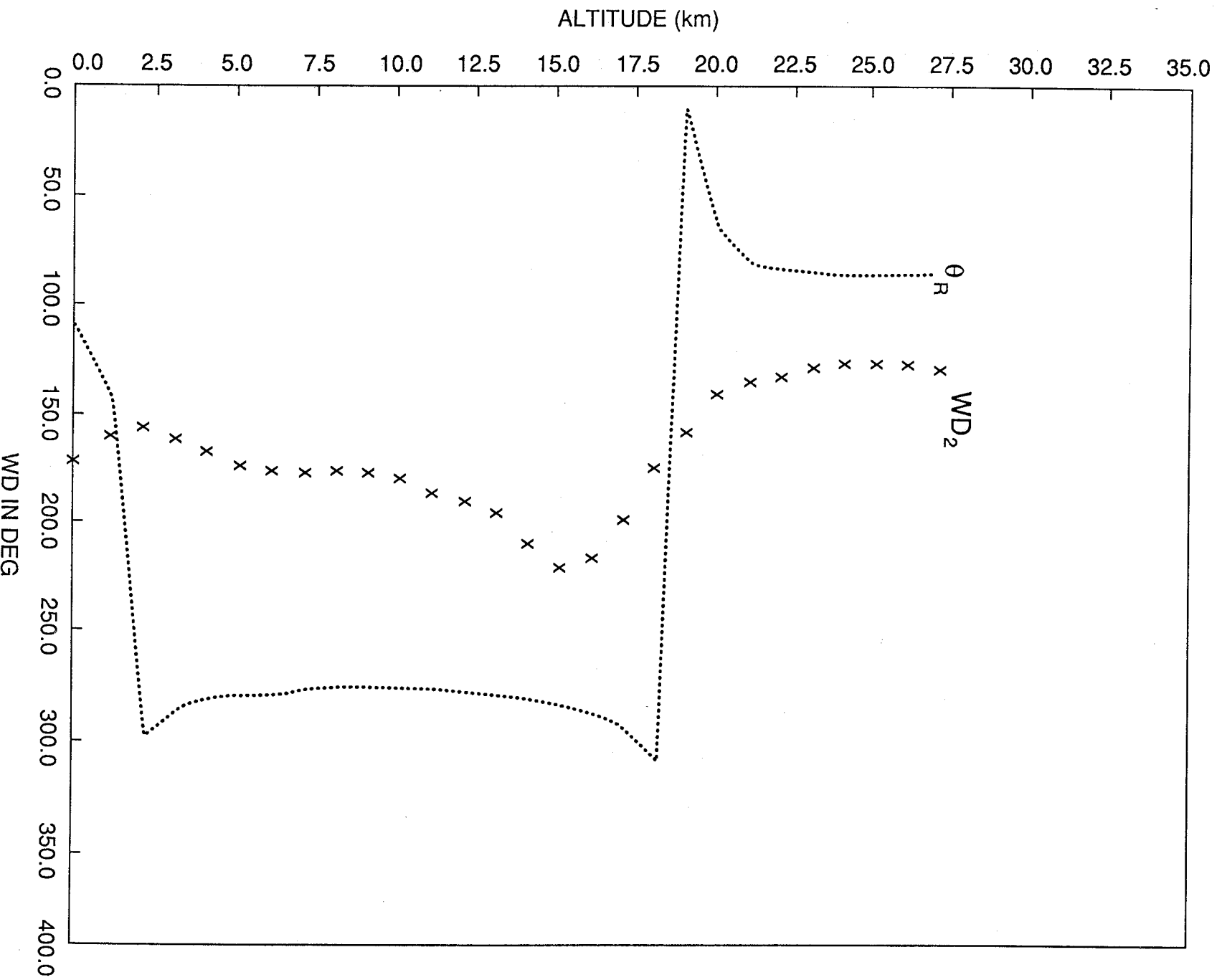85-percent probability ellipse, flight azimuth of 90°, May, KSC.

Figure B-4. Wind vector profile components to the second semi-minor axis to the
85-percent probability ellipse, flight azimuth of 90°, May, KSC.

Figure B-5. Wind speed to the first semi-major axis to the 85-percent probability ellipse, flight azimuth of 90°, May, KSC.

Figure B-6. Wind direction to the first semi-major axis to the 85-percent probability ellipse, flight azimuth of 90°, May, KSC.
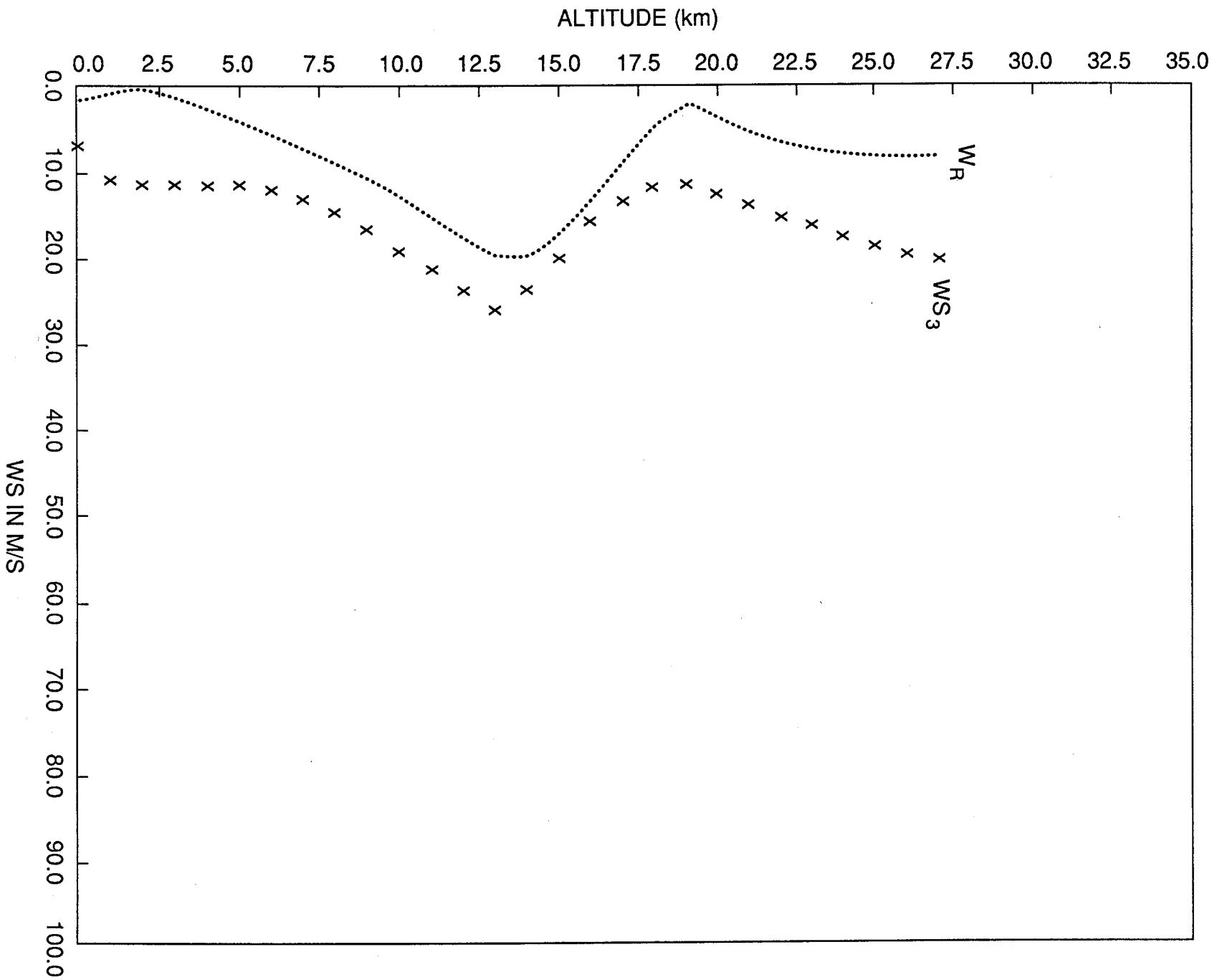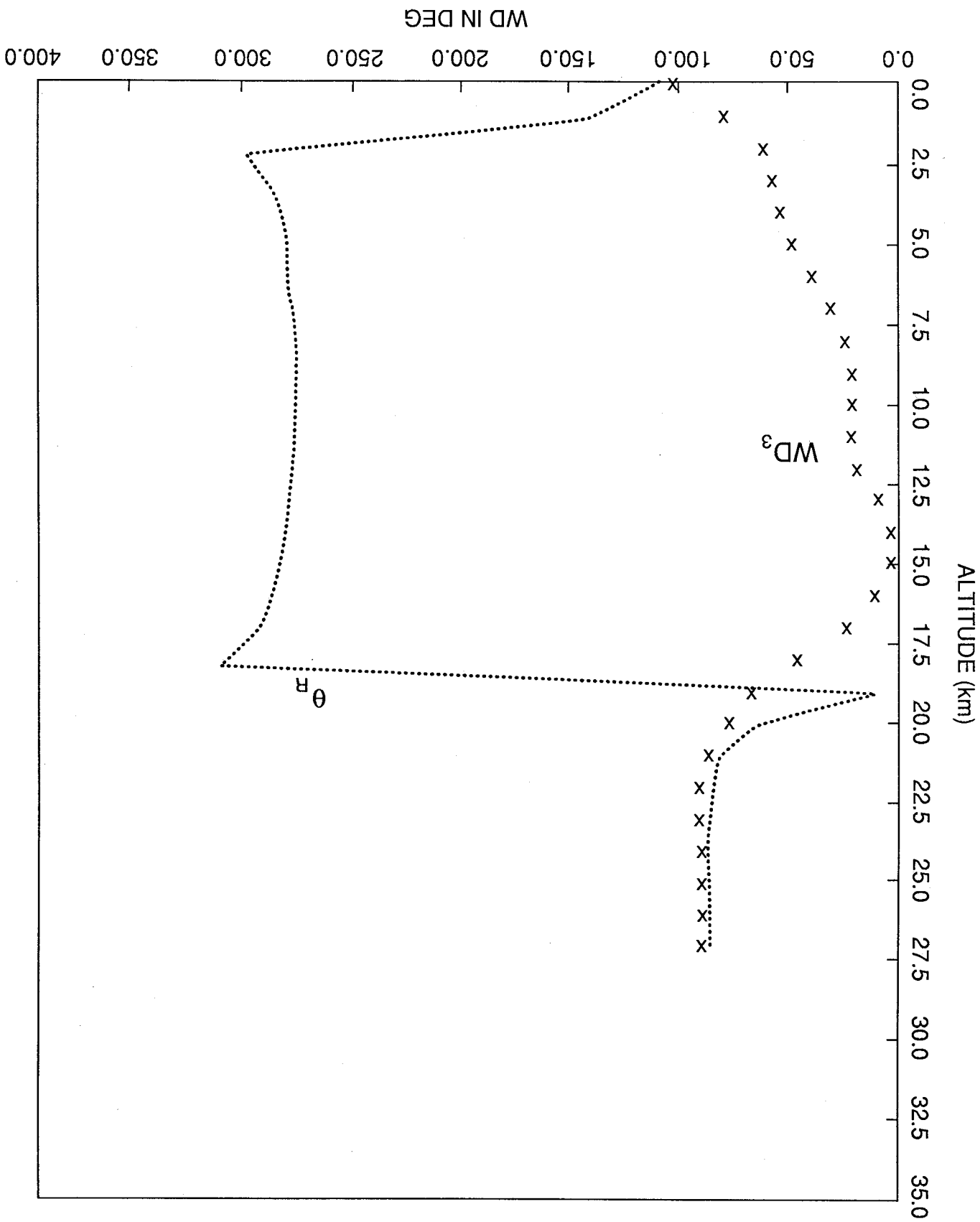
Figure B-7. Wind speed to the first semi-minor axis to the 85-percent probability ellipse, flight azimuth of 90°, May, KSC.

49

Figure B-8. Wind direction to the first semi-minor axis to the 85-percent probability ellipse, flight azimuth of 90°, May, KSC.

Figure B-9. Wind speed to the second semi-major axis to the 85-percent probability ellipse, flight azimuth of 90°, May, KSC.

Figure B-10. Wind direction to the second semi-major axis to the 85-percent probability ellipse, flight azimuth of 90°, May, KSC.
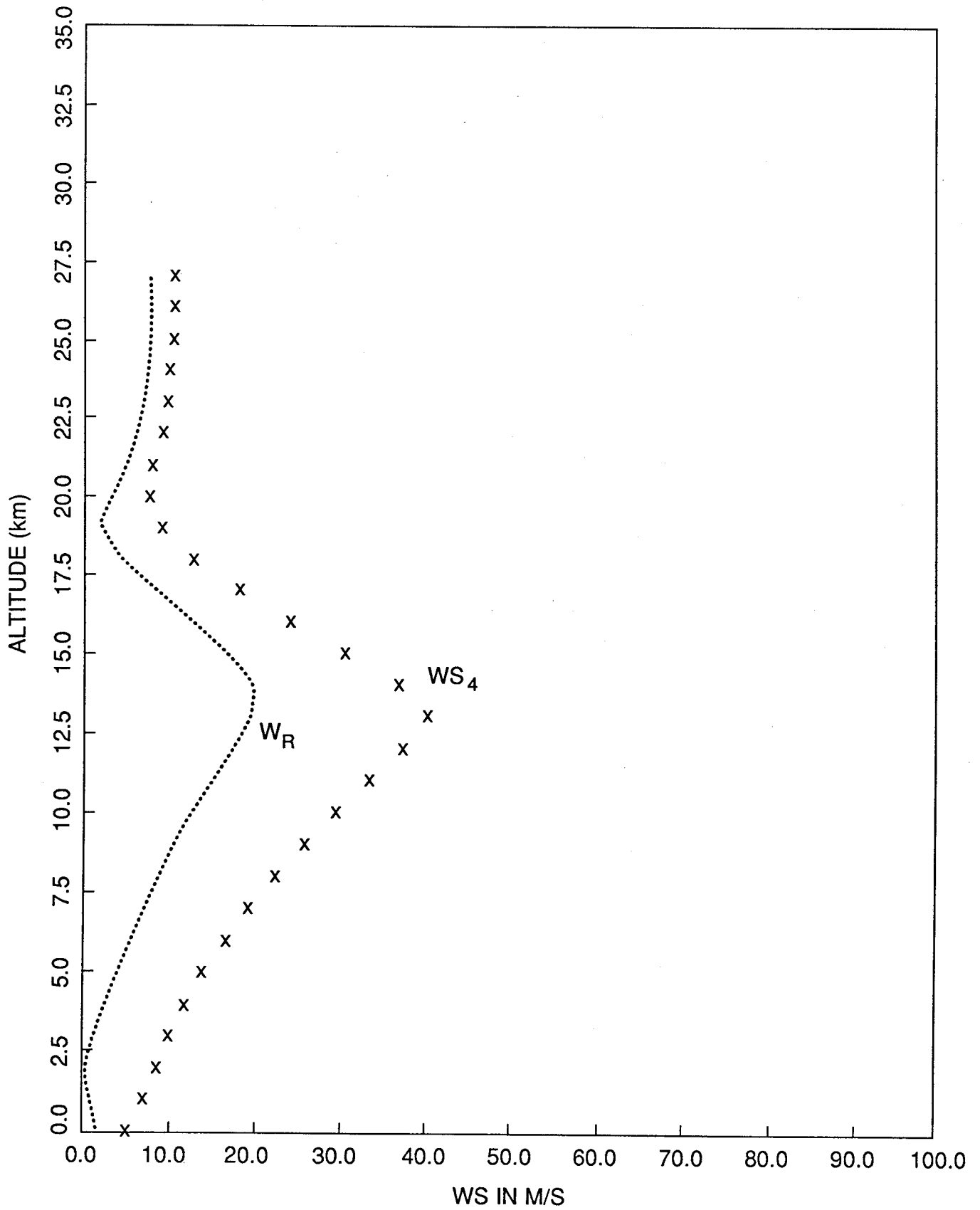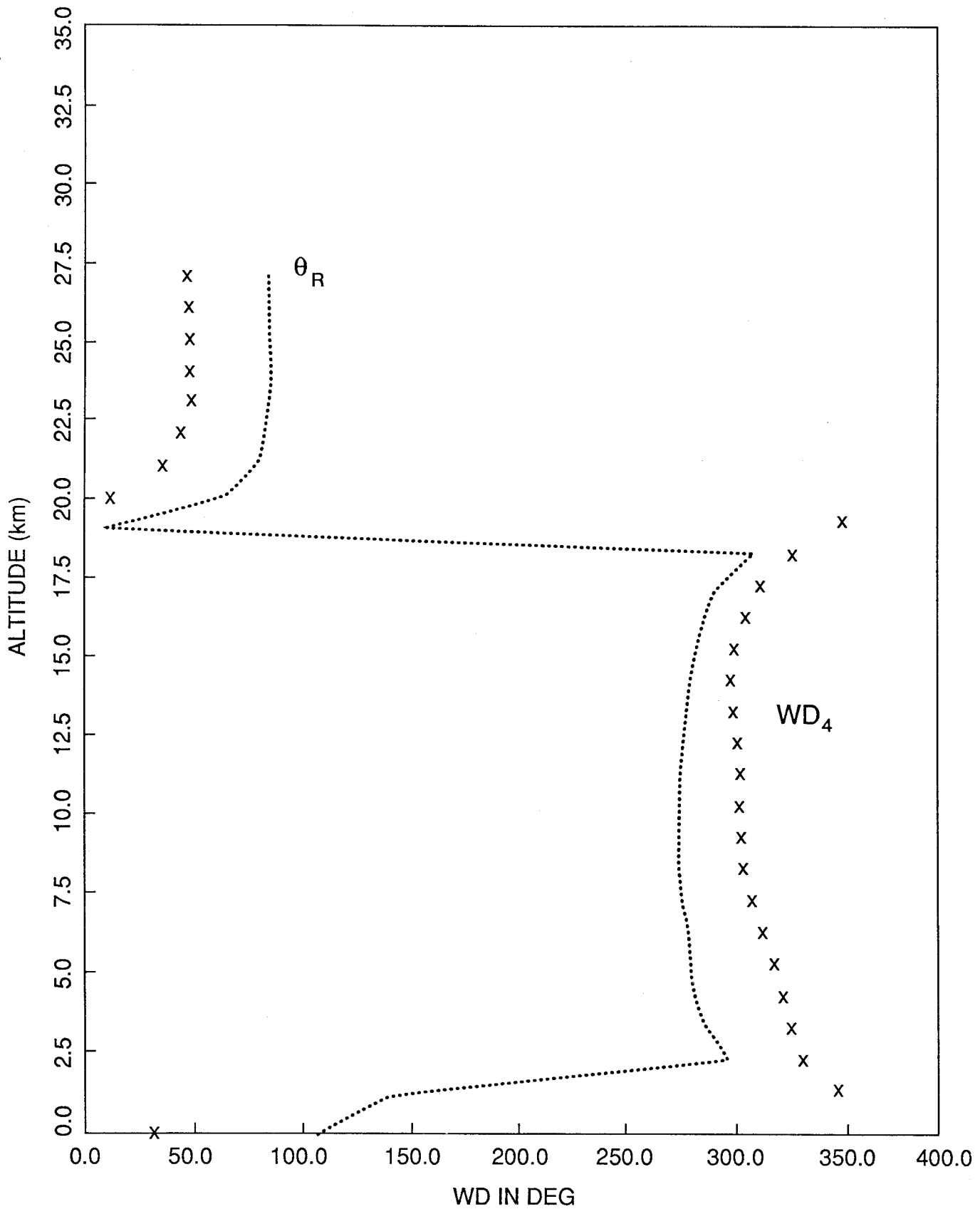
WD IN DEG

ALTITUDE (km)

WD₃

θ_R

Figure B-11. Wind speed to the second semi-minor axis to the 85-percent probability ellipse, flight azimuth of 90°, May, KSC.
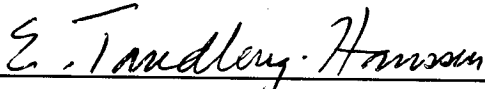
Figure B-12. Wind direction to the second semi-minor axis to the 85-percent probability ellipse, flight azimuth of 90°, May, KSC.

APPROVAL

WIND MODELS FOR THE NSTS ASCENT TRAJECTORY BIASING FOR WIND LOAD ALLEVIATION

By O.E. Smith, S.I. Adelfang, G.W. Batts, and C.K. Hill

The information in this report has been reviewed for technical content. Review of any information concerning Department of Defense or nuclear energy activities or programs has been made by the MSFC Security Classification Officer. This report, in its entirety, has been determined to be unclassified.

E. TANDBERG-HANSSEN
Director, Space Science Laboratory